Taxon-specific hydrogen isotope signals in cultures and mesocosms facilitate ecosystem and hydroclimate reconstruction

S. Nemiah Ladd[a, b]*, Daniel B. Nelson[b, c], Blake Matthews[d], Shannon Dyer[b], Romana Limberger[e,f], Antonia Klatt[a], Anita Narwani[g], Nathalie Dubois[h, i], Carsten J. Schubert[b, j]

[a] University of Basel, Department of Environmental Sciences, Basel, Switzerland

[b] Swiss Federal Institute of Aquatic Science and Technology (EAWAG), Department of Surface Waters – Research and Management, Kastanienbaum, Switzerland

[c] University of Basel, Department of Environmental Sciences – Botany, Basel, Switzerland

[d] Swiss Federal Institute of Aquatic Science and Technology (EAWAG), Department of Fish Ecology and Evolution, Kastanienbaum, Switzerland

[e] Swiss Federal Institute of Aquatic Science and Technology (EAWAG), Department of Aquatic Ecology, Kastanienbaum, Switzerland

[f] University of Zurich, Department of Evolutionary Biology and Environmental Studies, Zurich, Switzerland

[g] Swiss Federal Institute of Aquatic Science and Technology (EAWAG), Department of Aquatic Ecology, Dübendorf, Switzerland

[h] Swiss Federal Institute of Aquatic Science and Technology (EAWAG), Department of Surface Waters – Research and Management, Dübendorf, Switzerland

[i] Swiss Federal Institute of Technology (ETH-Zürich), Department of Earth Sciences, Zürich, Switzerland

[j] Swiss Federal Institute of Technology (ETH-Zürich), Department of Environmental Systems Science, Zürich, Switzerland

*Corresponding author: n.ladd@unibas.ch, +41 61 207 36 27

Co-author email addresses: daniel.nelson@unibas.ch, Blake.Matthews@eawag.ch, shannon.dyer15@gmail.com, romana.limberger@ieu.uzh.ch, antonia.klatt@unibas.ch, Anita.Narwani@eawag.ch, Nathalie.Dubois@eawag.ch, Carsten.Schubert@eawag.ch

This is an unformatted post-print of a manuscript that has now been published at *Geochimica et Cosmochimica Acta*. The formatted publication is available open access at https://doi.org/10.1016/j.gca.2024.12.002

Abstract

Phytoplankton play a key role in biogeochemical cycles, impacting atmospheric and aquatic chemistry, food webs, and water quality. However, it remains challenging to reconstruct changes in algal community composition throughout the geologic past, as existing proxies are suitable only for a subset of taxa and/or influenced by degradation. Here, we investigate if compound-specific hydrogen isotope ratios (δ^2H values) of common algal lipids can serve as (paleo)ecological indicators. First, we grew 20 species of algae – representing cyanobacteria, diatoms, dinoflagellates, green algae, and cryptomonads – in batch cultures under identical conditions and measured δ^2H values of their lipids. Despite identical source water δ^2H values, lipid δ^2H values ranged from -455 ‰ to -52 ‰, incorporating variability associated with chemical compound classes and taxonomic groups. In particular, green algae synthesized fatty acids with higher δ^2H values than other taxa, cyanobacteria synthesized phytol with relatively low δ^2H values, and diatoms synthesized sterols with higher δ^2H values than other eukaryotes. Second, we assessed how changes in algal community composition can affect net δ^2H values of common algal lipids in 20 experimental outdoor ponds, which were manipulated via nutrient loading, and the addition of macrophytes and mussels. High algal biomass in the ponds, which was mainly caused by cyanobacterial and green algal blooms, was associated with higher δ^2H values for generic fatty acids, relatively stable δ^2H values for phytol and the dinoflagellate biomarker dinostanol, and lower δ^2H values for the more cosmopolitan sterol stigmasterol. These results are consistent with expectations from our culture-based analyses, with both datasets indicating large taxon-specific changes that are unlikely to be driven by bacterial heterotrophy. This suggests that measuring δ^2H values of multiple lipids from sediment and calculating ^2H-offsets between them can resolve changes in algal community composition from changes in source water isotopes. With an appropriate

availability of sedimentary lipids, this approach could permit the reconstruction of both taxonomic variability and hydroclimate from diverse sedimentary systems.

Key words: algae, ecohydrology, hydrogen isotopes, lakes, lipid biomarkers, sediments

1. Introduction

Anthropogenic perturbations of carbon, nitrogen, and phosphorus cycling have had profound impacts on aquatic ecosystems, and both eutrophication and global warming have changed the composition and relative abundance of phytoplankton taxa in marine and freshwater systems over the past decades (Diaz and Rosenberg, 2008; Monchamp et al., 2018; Markelov et al., 2019). These changes in phytoplankton community composition subsequently impact nutrient cycling, food webs, and water quality within aquatic systems, including freshwater lakes (Rabalais et al., 2010; Hixson and Arts, 2016; Huisman et al., 2018). Contextualizing these changes in relation to natural climate and biogeochemical forcings, as well as in response to pre-industrial human impacts is important to better understand and predict the consequences of current human activities on aquatic systems (Haas et al., 2019; Nwosi et al., 2023).

Various sedimentological proxies are available to reconstruct past changes in algal ecology, each with its own strengths and limitations. Classical paleolimnological approaches involve counting fossilized remains of individual taxa, including diatom frustules, dinoflagellate cysts, and cyanobacterial akinetes (Livingstone and Jaworski, 1980; Stoermer et al., 1985; Dixit et al., 1992; Lotter, 1998; Gosling et al., 2020). While these microscopic analyses can provide a high degree of taxonomic precision, they are limited to organisms that produce suitable remains, and many ecologically important taxa including picocyanobacteria and most green algae are missing from such reconstructions. Recent advances in the analysis

of sedimentary ancient DNA (sedaDNA) also provide the opportunity for highly-resolved ecological reconstructions (Stoof-Leichsenring et al., 2015; Monchamp et al., 2018; Nwosi et al., 2023), but questions remain about biases introduced from selective preservation of DNA in the sediment and/or amplification of specific DNA fragments during sample processing (Pawlowski et al., 2017; Strivens et al., 2018; Vasselon et al., 2018; Thorpe et al., 2024), as well as the long-term applicability of sedaDNA on geologic time scales (Boere et al., 2011; Kirkpatrick et al., 2016). The relative distribution of pigments and lipid biomarkers in sediments are informative about changes in the abundance of broader algal taxonomic groups (Leavitt and Findlay, 1994; Schubert et al., 1998; Volkman, 2003; Naeher et al., 2012; McGowan et al., 2012; Bauersachs et al., 2017), but these analyses can also be affected by selective degradation (Leavitt and Hodgson, 2002; Bianchi et al., 2002; Reuss et al., 2005).

Another possible approach for reconstructing past changes in algal community structure is based on hydrogen isotopes of common algal lipids (δ^2H_{lipid} values), such as phytol, the side-chain moiety of chlorophyll, and the common membrane lipid $C_{16:0}$ fatty acid (palmitic acid). Hydrogen isotopes of these compounds and other, more source-specific lipid biomarkers, such as the dinoflagellate biomarker dinosterol, have primarily been investigated as proxies for the hydrogen isotopic composition of source water (δ^2H_{water} values) (Huang et al., 2004; Sachse et al., 2004; Sachse et al., 2012; Maloney et al., 2019; Weiss et al., 2019). Additionally, culturing and field studies have demonstrated that $^2H/^1H$ fractionation between lipids and source water ($\alpha^2H_{Lipid/Water}$ values) are sensitive to a variety of factors including salinity (Schouten et al., 2006; Sachse and Sachs, 2008; Nelson and Sachs, 2014), light availability (van der Meer et al., 2015; Sachs et al., 2017), growth rate (Schouten et al., 2006; Z. Zhang et al., 2009; Sachs and Kawka, 2015), and central metabolism (X. Zhang et al., 2009; Osburn et al., 2011; Heinzelmann et al., 2015; Wikjer et al., 2019; Cormier et al., 2022). However, in a limited number of laboratory studies where multiple species of algae

110 have been cultured under identical conditions, large differences in $\alpha^2H_{Lipid/Water}$ values have
111 been observed among different species (Sessions et al., 1999; Schouten et al., 2006; Zhang
112 and Sachs, 2007; Z. Zhang et al., 2009; Heinzelmann et al., 2015; Pilecky et al., 2024). Most
113 of these investigations included only a small number of species, and were not designed to
114 specifically determine how δ^2H_{lipid} values differ among algal taxonomic groups. Recent work
115 by Pilecky et al. (2024) demonstrated that differences in $\alpha^2H_{Fatty\ Acid/Water}$ values among taxa
116 are large relative to plausible changes in δ^2H_{water} values in natural settings, but only
117 considered fatty acids and not phytol or sterols, compounds that are also found in significant
118 quantities in algal biomass and that are frequently attributed to phytoplankton sources in
119 sediment.
120 Empirical calibrations of the relationship between algal δ^2H_{lipid} values and δ^2H_{water}
121 values in natural systems have also frequently observed large variability in apparent
122 hydrogen isotope fractionation (e.g., Nelson and Sachs., 2014; Ladd et al., 2017; Ladd et al.,
123 2018; Ladd et al., 2021a). This variability differs in magnitude and, in some cases, in sign
124 among lipids of different compound classes, which could be due to differences in the types of
125 algae contributing lipids to sediments (Ladd et al., 2018; Ladd et al., 2021a). This suggestion
126 has not yet been systematically evaluated, but if δ^2H_{lipid} values consistently vary among algae
127 taxonomic groups, it would facilitate reconstructions of past changes in algal community
128 composition, as these ubiquitous compounds are found in diverse sedimentary archives
129 (Meyers, 1997; Casteñada and Schouten, 2011; Witkowski et al., 2018). In particular,
130 comparing changes in relative offsets among δ^2H_{lipid} values from different compound classes
131 could allow changes in community composition to be assessed independently from changes
132 in δ^2H_{water} values. Another key advantage of this approach in the context of paleoecology is
133 that isotopic composition of hydrogen bound to carbon is stable at the temperatures and

pressures found near Earth's surface and sedimentary deposits prior to catagenesis (Schimmelmann et al., 2006).

To investigate how hydrogen isotope fractionation for diverse lipids varies among different types of algae, we grew 20 different species of algae, representing five taxonomic groups, under identical conditions and measured the δ^2H values of each lipid they produced in high quantities. We focused on lipids that are prominent in algal biomass and also frequently found in diverse sedimentary systems, and considered differences in compounds synthesized through distinct biochemical pathways. We then evaluated how differences in algal community structure, observed in 20 outdoor experimental ponds (15000 L), can be translated into net δ^2H_{lipid} values of common and source-specific specific lipids recovered from suspended particles. We use the results of these laboratory and outdoor experiments to present a conceptual framework for how algal δ^2H_{lipid} values can be combined with δ^2H values from other biomarkers co-occurring in sediment samples to disentangle ecological and hydroclimatic signals.

2. Methods

2.1 Phytoplankton cultures

We grew 20 species of phytoplankton (**Table S1**) in batch cultures at Eawag in Kastanienbaum, Switzerland, in 1 L Erlenmeyer flasks at 15 °C under a 12-hour light/dark cycle. Light intensity ranged from 130 - 230 μmol m^{-2} s^{-1} depending on the proximity to the light bank, but culture locations were rotated daily to promote more uniform light distribution among cultures. All cultures were grown on WC medium (Guillard and Lorenzen, 1972), which we prepared from stock nutrient solutions. After the medium for each flask was prepared, we adjusted the pH to 7 and then autoclaved prior to inoculation. We inoculated new cultures from established cultures growing under identical conditions. Periodic

159 microscopy checks confirmed that cultures were unialgal, but not axenic. We monitored cell
160 density on alternating days by removing small volume test aliquots from each culture under
161 sterile conditions and then analyzing by flow cytometry (BD Accuri C6, BD Biosciences,
162 San Jose, CA, USA). We determined cell density at the transition to stationary phase with
163 initial cultures of each species, and then harvested individual cultures during the late
164 exponential growth stage when they were approaching this cell density. Cultures were
165 harvested by filtering them onto 142 mm diameter, 0.7 μm pore-size Whatman® GF/F glass
166 fiber filters (previously combusted at 450 °C), which were stored at -20 °C until analyses
167 were performed. We collected water samples for later analysis of the medium water δ^2H and
168 $\delta^{18}O$ values on alternating days under the same conditions used to collect cell density
169 aliquots.
170
171 *2.2 Experimental Ponds*
172 We collected experimental pond samples as part of a large-scale eutrophication
173 experiment that was designed to test the impact of nutrient loading perturbations on
174 interactions between algae, macrophytes, and mussels. This experiment was conducted at the
175 Eawag Experimental Ponds facility in Dübendorf, Switzerland in 2016 (47.405 °N, 8.609
176 °E), and has previously been described in more detail (Narwani et al., 2019; Lürig et al.,
177 2021). Each of the 20 artificial ponds used in the experiment had a volume of 15,000 L, a
178 maximum depth of 1.5 m, and was inoculated with an algal community derived from surface
179 waters of a nearby lake, Greifensee (47.354 °N, 8.672 °E). We randomly assigned the 20
180 ponds into five treatments (i.e., four ponds per treatment). Four ponds received neither
181 nutrients, macrophytes, nor mussels (i.e., oligotrophic controls). The remaining 16 ponds
182 received the same nutrient loading treatment over the course of the experiment (Narwani et
183 al., 2019; Lürig et al., 2021), and, at the initiation of the experiment, four ponds

184 received Macrophytes (*Myriophillum spicatum*), four ponds received mussels (*Dreissena*
185 *polymorpha*), four ponds received both macrophytes and mussels, and four ponds received
186 neither macrophytes nor mussels (control ponds with nutrients). Nitrate and phosphate were
187 added in the form of KNO_3 and K_2HPO_4 at double the Redfield Ratio (N:P = 32:1), and as
188 pulses of increasing P concentration over time: 10 µg/L (August 12th), then 20 µg/L (August
189 26th), 30 µg/L (September 9th), and finally 40 µg/L (September 22nd, 2016).
190 On August 23rd, September 13th, and October 5th, 2016, we collected 15 L of water
191 from each pond, using a PVC tube (5 cm diameter, 180 cm length) equipped with a stopper
192 and pull-cord, which allowed the entire water column to be sampled. To prevent cross-
193 contamination during sampling, each pond had its own PVC tube sampler and water
194 collection bucket. Water was filtered through identical filters to those used for batch cultures
195 until either the entire 15 L had been filtered, or until the filter clogged. Filters were stored
196 frozen at -20 °C prior to freeze-drying. We also collected 8 mL of filtered water for isotopic
197 analysis from each pond on each sampling date. Water samples were stored in the dark at
198 room temperature in glass screw-cap vials that were sealed with electrical tape.
199 Throughout the summer and fall, depth-integrated pond water was collected using the
200 same PVC tubes every week, along with samples for chlorophyll concentrations and algal
201 cell counts (Narwani et al., 2019). Methodology for these analyses and resulting data were
202 published by Narwani et al. (2019).
203
204 *2.3 Lipid processing*
205 We extracted and purified lipids from all samples following previously described
206 protocols (Ladd et al., 2017; Ladd et al., 2021b). In brief, freeze-dried filters were microwave
207 extracted (SOLVpro, Anton Paar, Graz, Austria) in 9:1 dichloromethane (DCM)/methanol
208 (MeOH) at 70 °C and the resulting TLE was saponified in 1N KOH in MeOH (3 hours at 70

°C). We separated neutral lipids and fatty acids from each other by extracting the saponified sample with hexane, then acidifying it to pH < 2 and extracting again with hexane. We methylated fatty acids with 5 % HCl in MeOH (12 hours at 70 °C). We separated neutral lipids from pond samples into compound classes using silica gel column chromatography, and acetylated 95 % of the resulting alcohol fraction with acetic anhydride in pyridine (30 minutes at 70 °C). We acetylated 95 % of the neutral fraction from batch culture samples under identical conditions.

We quantified lipids by gas chromatography – flame ionization detection (GC-FID) (Shimazdu, Kyoto, Japan) at Eawag in Kastanienbaum, Switzerland, as described by Ladd et al. (2017). We used internal recovery standards (5α-cholestane, stearyl sterate, *n*-C_{19}-alkanol, $C_{19:0}$-alkanoic acid) that we quantitatively added prior to lipid extraction to account for any losses during sample handling. We identified fatty acids based on retention times relative to compounds in a fatty acid standard mixture (Supelco 37 component FAME mix, SigmaAldrich). We identified phytosterols and stanols from pond samples by gas chromatography – mass spectrometry (GC-MS) (Agilent Technologies, Santa Clara, CA, USA) at Eawag in Dübendorf, Switzerland, as described by Krentscher et al. (2019). In order to confirm compound identifications, we silylated the 5 % reserve aliquots of the alcohol fraction from each pond sample (25 µL BSTFA in 25 µL pyridine at 60 °C for 1 hour). We compared mass spectra from the resulting trimethylsilyl-ethers to published spectra, and used diagnostic fragments and relative peak areas to confirm identifications of acetylated alcohols, many of which did not have published reference spectra (**Table S2**). We identified acetylated sterols from algal cultures by GC-MS (Shimazdu, Kyoto, Japan) at Eawag in Kastanienbaum as described by Ladd et al (2017), comparing resulting mass spectra to those previously identified from pond samples.

234 *2.4 Lipid δ^2H measurements*

235 We measured compound specific hydrogen isotopes by gas chromatography–isotope
236 ratio mass spectrometry (GC-IRMS) at Eawag in Kastanienbaum on a Trace 1310 GC
237 coupled to a Delta V Plus IRMS with a ConFlow IV interface (Thermo Scientific, Waltham
238 MA, USA), following methods previously described by Ladd et al., (2018). We analyzed a
239 mix of *n*-alkanes (*n*-$C_{17, 19, 21, 23, 25, 28, 34}$) of known δ^2H values from Arndt Schimmelmann
240 (Indiana University) as reference materials in triplicate at the beginning and end of each
241 sequence, as well as after every 8-9 injections of samples. The *n*-alkane standards were
242 analyzed at a range of injection volumes throughout the sequence such that their peak sizes
243 spanned and exceeded the range of sample peak heights. All sample and standard compound
244 δ^2H values were initially calculated in the Isodat software platform relative to H_2 reference
245 gas. After measurement, the δ^2H values of the standards were used to reference the sample
246 compound δ^2H values to the VSMOW scale and to correct for isotope effects associated with
247 retention time, peak area, or time-based drift, using multiple linear regressions. We
248 determined the δ^2H value of H added during methylation by methylating phthalic acid with a
249 known δ^2H value (Arndt Schimmelmann, Indiana University) and approximated the δ^2H
250 value of H added during acetylation by measuring acetylated and unacetylated *n*-C_{10}-alkanol.
251 We used these δ^2H values and isotopic mass balance to correct for H added to analytes during
252 derivatization. We analyzed an additional quality control standard of *n*-C_{29} alkane three times
253 throughout each sequence (δ^2H = –139 ± 4.8 ‰; n = 98). The H_3^+ factor was calculated at the
254 beginning of each sequence and averaged 3.9 ± 0.4 during the analyses of culture samples
255 and 2.6 ± 0.1 during the analyses of pond samples.

256 We limited our analysis to compounds with peak areas greater than 15 Vs. Our analyses
257 were generally limited to compounds that produced baseline separated peaks at this
258 concentration on the GC-IRMS, with the exception being unsaturated C_{18} FAMEs, which

were manually integrated as a three-compound co-eluting peak, and subsequently referred to as $C_{18:x}$. In the pond samples, the presence and relative abundance of sterols, stanols, and FAMEs was highly variable among samples, and components that were suitable for compound-specific isotopic analyses according to our criteria were not consistent among samples.

2.5 Water isotope measurements

We filtered water samples through a 0.45 μm polyethersulfone membrane and analyzed their isotopic composition (δ^2H, $\delta^{18}O$) by cavity ring down spectroscopy (L-2120i Water Isotope Analyzer, Picarro, Santa Clara, CA) at ETH-Zürich as in Ladd et al. (2018). Chem correct software was actively used to flag samples with potential organic contamination. Average offsets from known values for standards analyzed with samples were 0.6 ‰ for hydrogen and 0.1 ‰ for oxygen. Average standard deviations for triplicate analyses were 0.7 ‰ for hydrogen and 0.09 ‰ for oxygen.

2.6 Calculations and Statistics

The hydrogen isotope ratios ($^2H/^1H$) of individual samples were normalized to the VSMOW scale and reported as δ^2H values, where $\delta^2H = (((^2H/^1H)_{sample}/(^2H/^1H)_{VSMOW})) - 1$, and is multiplied by 1000 to express in terms of ‰ (Coplen, 2011). The apparent $^2H/^1H$ fractionation factor between lipids and source water was calculated as $\alpha^2_{Lipid/Water} = (^2H/^1H)_{Lipid}/(^2H/^1H)_{Water}$ $(= (\delta^2H_{Lipid} + 1)/(\delta^2H_{Water} + 1))$. Because δ^2H_{water} values were consistent among batch cultures, we used the mean δ^2H value (-82.8 ± 0.7 ‰) to calculate $\alpha^2_{Lipid/Water}$ values from all cultures. Although $\alpha^2_{Lipid/Water}$ is the aggregate isotope effect of several biochemical steps and may differ due to kinetic isotope fractionation across a wide range of δ^2H_{water} values, it serves as a useful representation of apparent $^2H/^1H$ fractionation

(Sessions and Hayes, 2005; Zhang et al., 2014). The relative offset in δ^2H values among lipids was calculated as $\delta^2H_{Lipid\ 1/Lipid\ 2}$ (= $(^2H/^1H)_{Lipid\ 1}/(^2H/^1H)_{Lipid\ 2} - 1$), and is multiplied by 1000 to express in terms of ‰. While δ notation is not frequently used to describe isotopic differences between two measured substances, this aligns with the IUPAC guidelines for isotope notation (Coplen, 2011) and avoids implying that one substance is the product of the other, which is the case when fractionation factors are used to describe these offsets. It also correctly expresses isotopic differences between two substances without introducing biases due to the non-linear nature of the delta scale, as is the case for direct subtraction. Throughout this text, when δ^2H values are written with a single subscript, it indicates $^2H/^1H$ ratios normalized to VSMOW, while δ^2H values written with paired compounds in the subscript (e.g., $\delta^2H_{Sterol/Phytol}$) indicate differences in δ^2H values between the two compounds.

Comparisons of δ^2H_{lipid}, $\alpha^2_{lipid\text{-}water}$ values, and $\delta^2H_{Lipid\ 1/\ Lipid\ 2}$ values among taxonomic groups were made with Brown-Forsythe and Welch one-way ANOVA tests, with posthoc Dunnett's T3 multiple comparisons test to assess pairwise comparisons among taxonomic groups. Ordinary least squares regression was used to compare $\alpha^2_{lipid\text{-}water}$ values and $\delta^2H_{Lipid\ 1/\ Lipid\ 2}$ values from the ponds with chlorophyll *a* concentrations and the relative biovolumes of different algal taxonomic groups. All statistical analyses were performed in Prism (Version 9.5.1, GraphPad Software, LLC). All correlations and differences described in the results and discussion are significant at the 0.05 confidence level unless explicitly stated otherwise.

3. Results

3.1 Hydrogen isotope fractionation in algal cultures varies among compound classes and taxonomic groups

The variability in δ^2H values for individual lipids among different cultures was large, even though δ^2H_{water} values were constant, indicating a wide range of species-specific $\alpha^2_{Lipid/Water}$ values (**Figure 1**). $\alpha^2_{Lipid/Water}$ values clustered by taxonomic class, with green algae having higher $\alpha^2_{C16:0/Water}$ values than any other group (**Figure 1a**). Green algae also tended to produce relatively ^2H-enriched phytol, especially relative to phytol from cyanobacteria (**Figure 1b**). However, the difference in δ^2H_{Phytol} values between green algae and diatoms was less pronounced than the difference in their respective $\delta^2H_{C16:0}$ values, and dinoflagellates and cryptomonads had similar δ^2H_{Phytol} values to green algae (**Figure 1b**). In the case of sterols, those from diatoms were enriched in ^2H relative to all three other groups of eukaryotic phytoplankton (**Figure 1c**), in marked contrast to the relatively low $\alpha^2_{C16:0/Water}$ and $\alpha^2_{Phytol/Water}$ values from diatoms.

Among algal taxonomic groups, there were also clear differences in the relative $^2H/^1H$ offset among biomarkers from different compound classes ($\delta^2H_{Lipid\ 1/Lipid\ 2}$ values) (**Figure 1**). Green algae and cyanobacteria tended to have relatively high $\delta^2H_{C16:0/Phytol}$ values compared to the remaining eukaryotic algal groups (**Figure 1d**). While the difference in mean $\delta^2H_{C16:0/Phytol}$ values among groups was large (> 100 ‰), it was not significant. Diatoms tended to have the lowest $\delta^2H_{C16:0/Sterols}$ values of any group (although these were not different from cryptomonads), while green algae tended to have the highest (although these were not significantly different from those of dinoflagellates) (**Figure 1e**). Diatoms had the highest $\delta^2H_{Sterol/Phytol}$ and dinoflagellates had the lowest, with intermediate values for green algae and cryptomonads (**Figure 1f**). The overall magnitude of variability for $\delta^2H_{C16:0/Sterols}$ values among all eukaryotic taxa was roughly twice as large as that of $\delta^2H_{Sterol/Phytol}$ values.

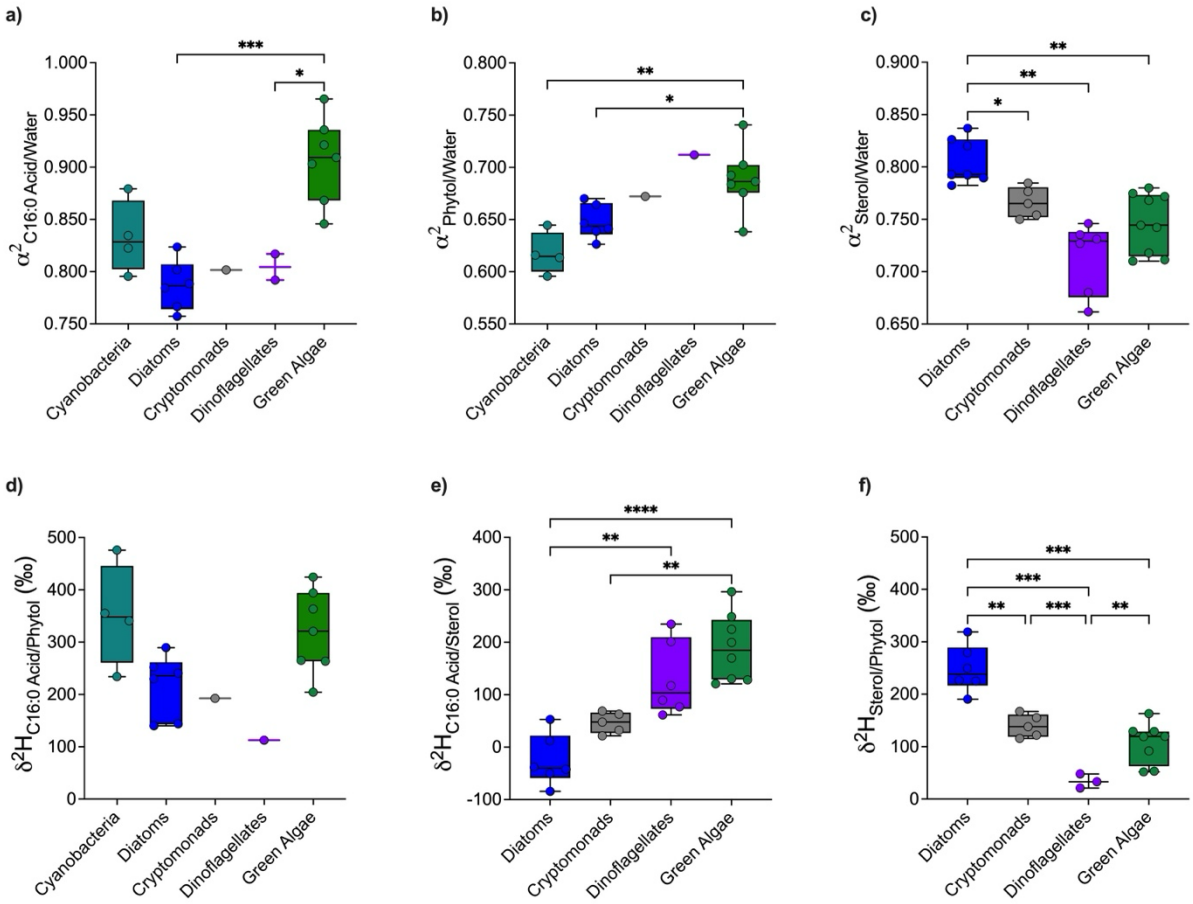

Figure 1 Hydrogen isotope variability among lipids from algal batch cultures. Panels a, b, and c show $\alpha^2_{Lipid/Water}$ values for C16:0 fatty acid, phytol, and all measured sterols, respectively. The y-axes of panels a, b, and c are scaled to span a range of 0.250, but the absolute values differ among panels to accommodate different $\alpha^2_{lipid/water}$ values for each compound. Panels d, e, and f show relative $^2H/^1H$ offsets ($\delta^2H_{Lipid\ 1/Lipid\ 2}$ values) between C16:0 fatty acid and phytol, C16:0 fatty acid and sterol, and sterols and phytol, respectively. The y-axes of panels d, e, and f are scaled to span a range of 500 ‰, but the absolute values differ among panels to accommodate different $\delta^2H_{Lipid\ 1/Lipid\ 2}$ values for each compound. $*p < 0.05$; $**p < 0.01$; $***p < 0.001$; $****p < 0.0001$.

3.2 Hydrogen isotope fractionation varied with nutrient additions to experimental ponds for some compounds

Pond water isotopes became progressively enriched in ^2H and ^{18}O as the experiment progressed due to evaporation, but had minimal variation among ponds each week (**Table 1**). Overall, δ^2H_{Water} values from the final sampling week were within ~ 10 ‰ of those from the first sampling week. Despite this relatively small range of δ^2H_{Water} values, δ^2H_{Lipid} values for individual compounds spanned a much larger range, > 150 ‰ in the case of some fatty acids.

The magnitude of variability in $\alpha^2_{Lipid/Water}$ values was not consistent among compounds, even for those we were able to measure in almost all samples. For example, the standard deviation for $\alpha^2_{C16:0\ Acid/Water}$ values was 0.043 (n = 58), while $\alpha^2_{Phytol/Water}$ values had a standard deviation of 0.012 (n = 53).

Table 1. Mean water isotope values for pond water during each sampling week (n = 20 for each week). Uncertainty represents one standard deviation of all measurements.

Date	δ^2H (VSMOW, ‰)	$\delta^{18}O$ (VSMOW, ‰)
23.08.2016	-37.4 ± 1.6	-3.4 ± 0.3
13.09.2016	-32.4 ± 0.9	-2.2 ± 0.2
05.10.2016	-29.9 ± 1.0	-1.7 ± 0.2

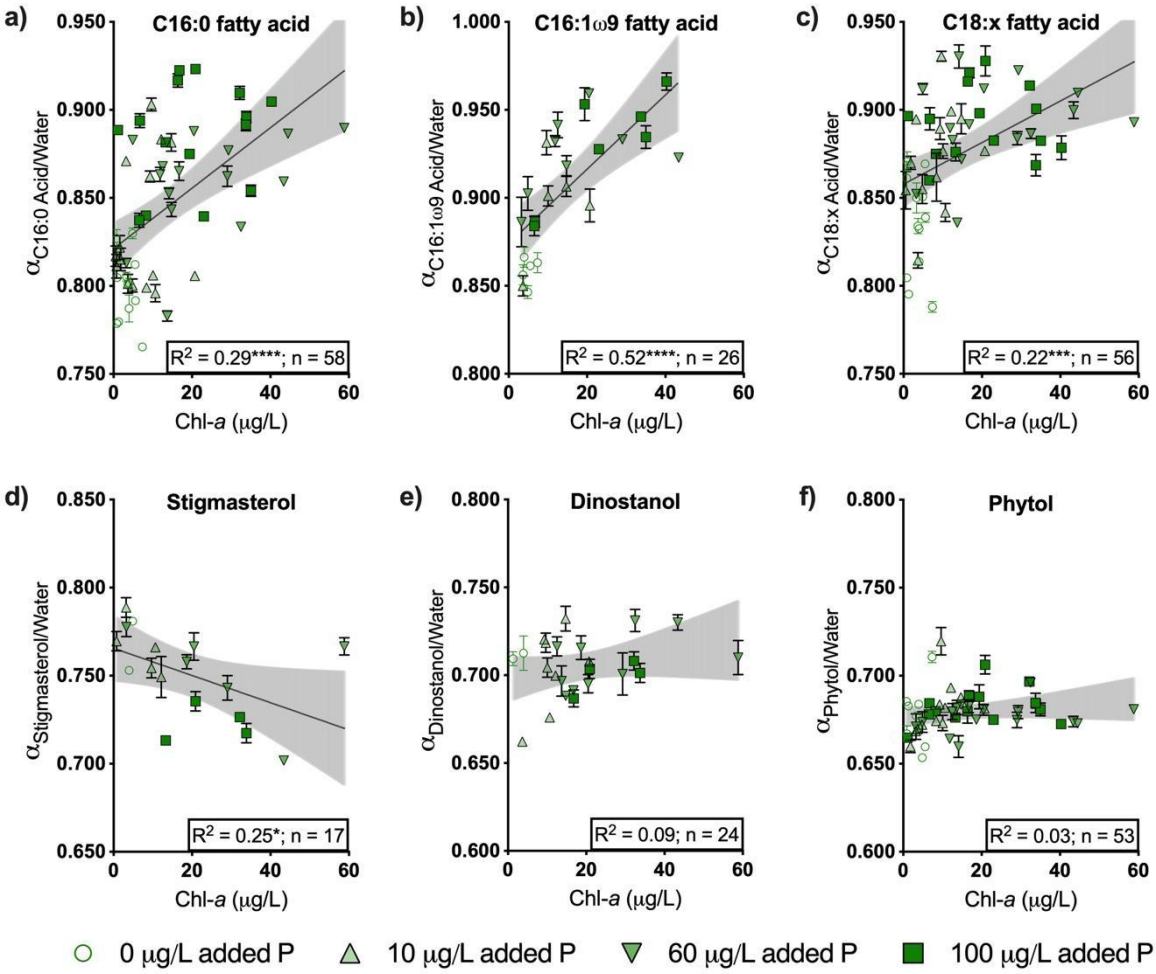

Figure 2 Relationships between $\alpha^2_{Lipid/Water}$ values and chlorophyll *a* concentration in experimental ponds for selected compounds. Symbols represent total cumulative added P. Ponds that were designated oligotrophic controls (0 µg/L added P) are represented with open

circles regardless of sampling week. For all other treatments, upward-facing triangles represent samples collected on August 23rd, downward-facing triangles represent samples collected on September 13, and squares represent samples collected on October 5, 2016. Shading represents 95 % confidence intervals of linear regressions. Regression lines are shown for significant linear correlations. *$p < 0.05$; ***$p < 0.001$; ****$p < 0.0001$.

For several compounds, including more generic fatty acids such as $C_{16:0}$, $C_{16:1}$, and $C_{18:x}$, $\alpha^2_{Lipid/Water}$ values were positively correlated with overall algal productivity in the pond experiment, as indicated by chlorophyll *a* concentration (**Figure 2**). In contrast to these fatty acids, $\alpha^2_{Lipid/Water}$ values for stigmasterol, the sterol which we were able to measure δ^2H values from in the greatest number of ponds, were negatively correlated with algal productivity. For other compounds, including phytol and the dinoflagellate biomarker dinostanol, there was no correlation between $\alpha^2_{Lipid/Water}$ values and productivity indicators (**Figure 2**).

In the experimental ponds, nutrient loading and the presence or absence of keystone species not only caused overall algal productivity to vary, but also resulted in changes in the relative abundance of different algal taxa, as explored in more detail by Narwani et al. (2019). In many cases, $\delta^2H_{Lipid\ 1/Lipid\ 2}$ values varied with changes in algal community composition that were consistent with the results of the unialgal batch cultures. For example, in ponds where the algal biovolume was dominated by cyanobacteria and/or green algae, $\delta^2H_{C16:0/Phytol}$ values were higher than in ponds where these two taxa were less abundant (**Figure 3a**), consistent with the pattern identified in the batch cultures (Figure 1d). Likewise, $\delta^2H_{C16:0/Stigmasterol}$ values were positively correlated with the relative abundance of green algae (**Figure 3b**), again, consistent with the batch cultures (**Figure 1e**). There was a negative trend for $\delta^2H_{Stigmasterol/Phytol}$ values as the relative abundance of green algae increased, but this correlation was not significant (**Figure 3c**).

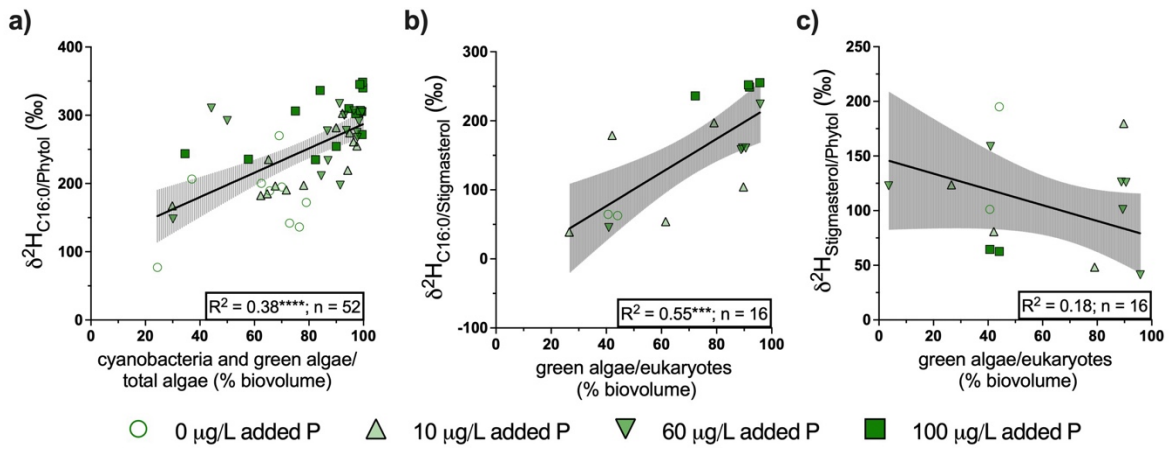

Figure 3 Relationships between $\delta^2H_{Lipid\ 1/Lipid\ 2}$ values and changes in the relative abundance of algal groups for selected compound pairs. Panel a shows the relationship between $\delta^2H_{C16:0/Phytol}$ values and the relative abundance of cyanobacteria and green algae (as a percentage of the total algal biovolume). Panel b shows the relationship between $\delta^2H_{C16:0/Stigmasterol}$ values and the relative abundance of green algae (as a percentage of the total eukaryotic algal biovolume), panel c shows the equivalent relationship for $\delta^2H_{Stigmasterol/Phytol}$ values (note different scaling for y-axis in panel c). Cyanobacteria are excluded from the biovolume in panels b and c because they do not produce sterols. Symbols represent total cumulative added P. Ponds that were designated oligotrophic controls (0 μg/L added P) are represented with open circles regardless of sampling week. For all other treatments, upward-facing triangles represent samples collected on August 23rd, downward-facing triangles represent samples collected on September 13, and squares represent samples collected on October 5, 2016. Shading represents 95 % confidence intervals of linear regressions; regression lines are only shown for significant correlations. ***$p < 0.001$, ****$p < 0.0001$.

4. Discussion

We determined how hydrogen isotope fractionation between lipids and source water varied among algae in batch cultures of 20 species representing five taxonomic groups, and assessed how changes in algal community composition in experimental ponds related to changes in net hydrogen isotope fractionation for both ubiquitous and relatively source-specific lipids. Our results indicate that variability in biosynthetic hydrogen isotope fractionation is large compared to the natural variability of hydrogen isotopes in the global water cycle. They also suggest that there are systematic differences in biosynthetic hydrogen isotope fractionation among algal taxonomic groups that differ among lipid compound classes. In the following discussion, we explore potential biochemical mechanisms that may

account for these patterns, demonstrate how the relative abundance of different algal species can affect the net hydrogen isotope signal recorded by ubiquitous algal lipids, and propose a conceptual framework for disentangling changes in algal community composition from changes in source water hydrogen isotopes in sedimentary records.

4.1 Sources of variability in hydrogen isotope fractionation factors among algal taxa

Many of the differences in $\alpha^2_{Lipid/Water}$ values for phytol and sterols that we observed among algal taxonomic groups in batch cultures are consistent with existing knowledge about sources of variability in biosynthetic hydrogen isotope fractionation during the synthesis of isoprenoid lipids. Although the hydrogen in the lipids of photosynthesizing organisms is originally from the water in which they grew, various biochemical reactions result in $^2H/^1H$ fractionation and impact the overall δ^2H values of lipids (Sessions et al., 1999; Session and Hayes, 2005; Sachse et al., 2012). In particular, contributions from NADPH produced by different reactions have a large influence on lipid δ^2H values (X. Zhang et al., 2009; Cormier et al., 2018; Wijker et al., 2019). NADPH produced in photosystem 1 in the chloroplast is depleted in ^2H by several hundred ‰ relative to NAD(P)H formed during glycolysis or by the oxidative pentose phosphate cycle (Schmidt et al., 2003; X. Zhang et al. 2009; Cormier et al., 2018). As such, processes that impact the relative contributions of hydride from distinct NADPH sources represent one of the main mechanisms by which biosynthetic $\alpha^2_{Lipid/Water}$ values can vary on large scales (Sachs and Kakwa, 2015; Maloney et al., 2016; Cormier et al., 2018; Ladd et al., 2021b).

The relative amount of H sourced from photosynthetic NADPH may be responsible for the commonly observed ^2H depletion of phytol relative to sterols from the same organism (**Figure 1**; Sessions et al., 1999; Chikaraishi et al., 2004; Sessions, 2006; Zhou et al., 2011; Ladd et al., 2018, 2021b). The isoprene building blocks of phytol are produced via the

methylerythritol phosphate (MEP) pathway in the plastid, most likely leading to the incorporation of relatively more H from photosynthetic NADPH than for isoprenoids produced via the mevalonic acid (MVA) pathway, which takes place in the cytosol (**Figure 4**; Sessions et al., 1999; Chikaraishi et al., 2004; Sessions, 2006; Zhou et al., 2011; Ladd et al., 2021b; Rhim et al., in press). Although sterols tend to be produced by the MVA pathway and phytol by the MEP pathway, they both contain common biosynthetic precursors that can be produced by both pathways, and that are likely exchanged across the plastid membrane (**Figure 4**) (Hemerlin et al., 2012; Ladd et al., 2021b, 2023).

Previous observations of variability in $\alpha^2_{Lipid/Water}$ values for phytol and sterols have frequently been attributed to potential exchange of isoprenoid precursors between these two pathways (Sachse et al., 2012; Maloney et al., 2016; Sachs et al., 2016, 2017; Ladd et al., 2018, 2021b). We suggest that the relatively low $\alpha^2_{Sterol/Water}$ values in green algae are due to the fact that they produce sterols via the MEP pathway and lack the MVA pathway, in contrast to all other eukaryotic algae, which produce isoprenoids using both the MVA and the MEP pathways (Schwender et al., 1996; Disch et al., 1998; Lichtenthaler, 1999). Therefore, green algae would be expected to have lower $\alpha^2_{Sterol/Water}$ values than other eukaryotic algae, consistent with the results of our batch cultures, where green algae had significantly lower $\alpha^2_{Sterol/Water}$ values than diatoms (**Figure 1c**).

Dinoflagellates in our cultures also had relatively low $\alpha^2_{Sterol/Water}$ values (**Figure 1c**), even though they have the genetic capability to produce sterols through the MVA pathway (Hemerlin et al., 2012). However, transcriptomic data indicate that many dinoflagellates rely exclusively on the MEP pathway for isoprenoid synthesis (Bentlage et al., 2016). Low $\alpha^2_{Sterol/Water}$ values for dinosterol and other sterols produced by dinoflagellates are consistent with a tendency for dinoflagellates to produce sterols via the MEP pathway, resulting in $\alpha^2_{Sterol/Water}$ values that are comparable to those from green algae, which are obliged to use the

462 MEP pathway for sterol synthesis. The low $\alpha^2_{Sterol/Water}$ values observed in our dinoflagellate
463 cultures are consistent with values for the dinoflagellate biomarker dinostanol in the pond
464 samples (**Figure 2**), as well as with those reported from environmental dinosterol (Nelson
465 and Sachs, 2014; Schwab et al., 2015; Maloney et al., 2019), a sterol primarily produced by
466 dinoflagellates (Volkman, 2003). For example, in surface sediments and suspended organic
467 matter filtered from the water column of saline and hypersaline lakes, $\alpha^2_{Dinosterol/Water}$ values
468 were consistently lower than $\alpha^2_{Brassicasterol/Water}$ values from the same samples (Nelson and
469 Sachs, 2014). The freshwater end member value for $\alpha^2_{Dinosterol/Water}$ in this study was 0.688,
470 which is within the range we observed for dinoflagellates in our cultures (**Figure 1c**) and
471 similar to measurements of $\alpha^2_{Dinosterol/Water}$ from suspended organic matter in lakes in
472 Cameroon (0.713 ± 0.011; Schwab et al., 2015). These low $\alpha^2_{Sterol/Water}$ values for sterols
473 produced by dinoflagellates, along with expression of MEP genes but not MVA genes in
474 several dinoflagellate taxa (Bentlage et al., 2016), provide additional support for the
475 hypothesis that relative use of the MEP pathway for sterol precursors is a primary driver of
476 variability in $\alpha^2_{Sterol/Water}$ values.
477

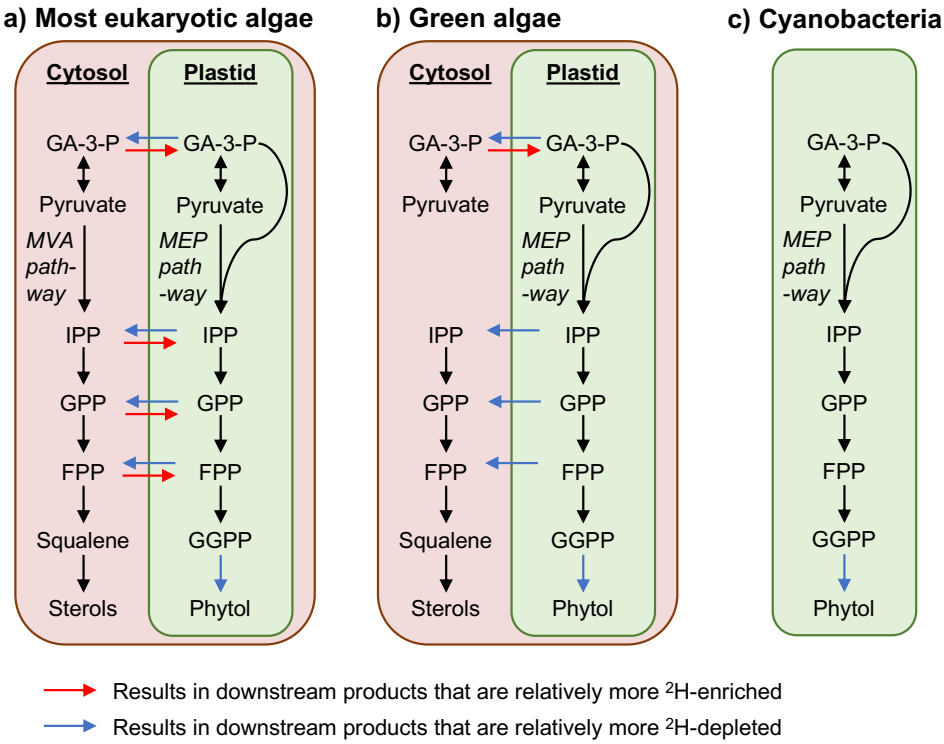

Figure 4: Schematic representation of biochemical steps that could result in ^{2}H-enrichment or depletion for isoprenoid lipids in (a) eukaryotic microalgae other than green algae, (b) green algae, and (c) cyanobacteria. Several intermediate compounds are omitted for clarity. Abbreviations: FPP, farnesyl pyrophosphate; GA-3-P, glyceraldehyde 3-phosphate; GGPP, geranylgeranyl pyrophosphate; GPP, geranyl pyrophosphate; IPP isopentenyl pyrophosphate; MEP, methylerythritol phosphate; MVA, mevalonic acid.

In contrast to sterols, phytol is typically produced via the MEP pathway (Hemerlin et al., 2012) (**Figure 4**). Low $\alpha^{2}_{Phytol/Water}$ values, relative to those from sterols and other isoprenoids, are typically attributed to phytol's MEP source (Sessions et al., 1999; Sessions, 2006; Ladd et al., 2021b). Our algal cultures and experimental pond samples were also characterized by low $\alpha^{2}_{Phytol/Water}$ values (**Figure 1b, 2f**). Notably, $\alpha^{2}_{Phytol/Water}$ values were always lower than $\alpha^{2}_{Sterol/Water}$ values from the same sample, indicated by positive $\delta^{2}H_{Sterol/Phytol}$ values. This relationship is observed even for cultures of taxa that cannot (green algae) or apparently do not (dinoflagellates) produce sterols via the MVA pathway (**Figure 1f**). Therefore, low $\alpha^{2}_{Phytol/Water}$ values cannot be attributed solely to phytol's production in the MEP pathway. Additional ^{2}H-depletion of phytol relative to MEP-derived sterols is likely

caused by the addition of extremely ^{2}H-depleted hydrogen during the hydrogenation of geranylgeranyl pyrophosphate (GGPP) to form phytol (Chikaraishi et al., 2009) (**Figure 4**). The only reported $\delta^{2}H_{GGPP/Phytol}$ values are from cucumber cotyledons, and have a value of +98 ‰ (Chikaraishi et al., 2009), comparable to $\delta^{2}H_{Sterol/Phytol}$ values of +89 ± 53 ‰ from cultured green algae and dinoflagellates, and to $\delta^{2}H_{Sterol/Phytol}$ values of ~ +85 ‰ from higher plants that produce sterols primarily with MEP-derived precursors (Ladd et al., 2021b). As such, differences between sterol and phytol δ^{2}H values (as non-zero $\delta^{2}H_{Sterol/Phytol}$ values) from green algae and dinoflagellates are likely caused only by hydrogenation of GGPP to phytol, while the higher $\delta^{2}H_{Sterol/Phytol}$ values from cultured diatoms (+221 ± 47 ‰) likely represent the combined H-isotope effects of GGPP hydrogenation and sterol synthesis via the MVA pathway (**Figure 4**).

The lowest $\alpha^{2}_{Phytol/Water}$ values observed in our cultures were from cyanobacteria (**Figure 1b**). Cyanobacteria only produce isoprenoids via the MEP pathway and lack the MVA pathway, therefore there is no possibility that cyanobacterial phytol is synthesized from MVA intermediates. In most eukaryotic algae, metabolic cross-talk of isoprenoid intermediates across the plastid membrane has the potential to contribute relatively ^{2}H-enriched precursors to phytol synthesis, as a significant portion of phytol in higher plants can be from MVA-derived precursors (Opitz et al., 2014), and the same is likely true for phytol in eukaryotic algae that maintain both pathways. However, crosstalk between the MEP and MVA pathways cannot explain why green algae also produce phytol that is enriched in ^{2}H relative to phytol from cyanobacteria, since these eukaryotes also lack the MVA pathway. Another possible mechanism by which ^{2}H-enriched cytosolic precursors could be incorporated into phytol in eukaryotes is via transport of glyceraldehyde 3-phospate (GA-3-P) into the plastid, where it could substitute for relatively ^{2}H-depleted GA-3-P produced from the Calvin Cycle (**Figure 4**) (Yáñez-Serrano et al., 2019; Kreuzwieser et al., 2021; Ladd et

al., 2021b). Incorporation of cytosolic GA-3-P into plastidic isoprenoids could explain ^{2}H-enrichment of phytol from all eukaryotes relative to phytol from cyanobacteria, and thus seems like the more plausible explanation to account for this difference.

It is less apparent why fatty acid $\alpha^{2}_{\text{Fatty Acid/Water}}$ values would be higher in green algae than in other taxa (**Figure 1a**). Differences in the metabolism of green algae relative to diatoms and other eukaryotes, including the nature of their plastid membranes (Archibald, 2015; Zulu et al., 2018) and NADPH transfer between chloroplasts and mitochondria (Bailleul et al., 2015) could potentially shift the relative sources of carbohydrate precursors and/or NADPH used in fatty acid synthesis, thereby affecting overall $\alpha^{2}_{\text{Fatty Acid/Water}}$ values. An alternative possibility is that cultures with high $\alpha^{2}_{\text{Fatty Acid/Water}}$ values were impacted by fatty acids from heterotrophic bacteria, as these tend to produce fatty acids that are enriched in ^{2}H relative to those from photoautotrophs (X. Zhang et al., 2009; Heinzelmann et al., 2016). In order to increase $\alpha^{2}_{\text{Fatty Acid/Water}}$ values from 0.800 to 0.96, roughly the range observed across our cultures, isotopic mass balance indicates that 40 % of fatty acids would need to be from heterotrophic bacteria with an average $\alpha^{2}_{\text{Fatty Acid/Water}}$ value of 1.200 (X. Zhang et al., 2009; Heinzelmann et al., 2016) if the algae had a consistent $\alpha^{2}_{\text{Fatty Acid/Water}}$ value of 0.800 across cultures. While the cultures were not axenic and small amounts of bacteria were present, this was not exclusive to green algal cultures with high $\alpha^{2}_{\text{Fatty Acid/Water}}$ values, and bacterial abundance never approached a level where they could have had a sizable impact on net $\alpha^{2}_{\text{Fatty Acid/Water}}$ values.

From our present data, we are only able to observe that this ^{2}H-enrichment of green algal fatty acids seems to be robust, with consistent $\alpha^{2}_{\text{Fatty Acid/Water}}$ values for green algal cultures and for ponds that became dominated by green algae. Adding confidence to this observation, similarly high $\alpha^{2}_{\text{Fatty Acid/Water}}$ values were recently reported from batch cultures of green algae grown at higher temperatures under a different light regime Pilecky et al.

(2024) (**Figure 5**). The similarities between our results and those of Pilecky et al. (2024) further support the conclusion that heterotrophic bacteria had minimal influence on net $\alpha^2_{Fatty\ Acid/Water}$ values in our batch cultures. Future experimental work should investigate the mechanistic causes of relatively ^{2}H-enriched fatty acids in green algae, relative to other taxa. Ideally, these follow-up experiments will incorporate complementary metabolomic and transcriptomic analyses, which could also be used to test the hypotheses we have presented for variable $\alpha^2_{Lipid/Water}$ values during isoprenoid synthesis by different taxonomic groups.

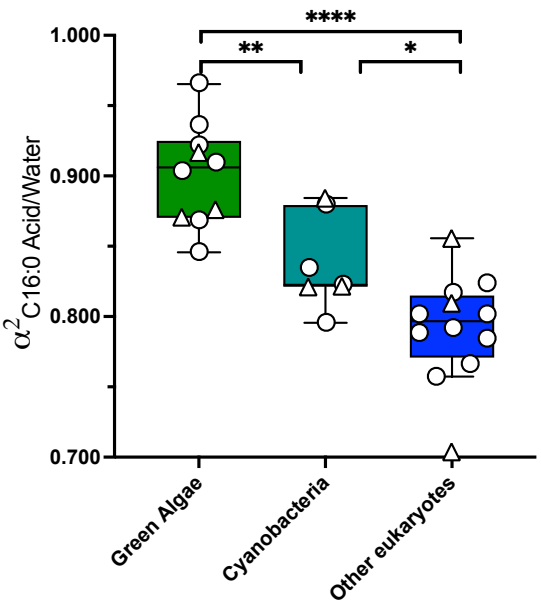

Figure 5: Combined $\alpha^2_{C16:0/Water}$ values from batch cultures in our study (open circles) and those of Pilecky et al. (2024; filled triangles). Box plots and one-way ANOVA results are shown for the combined dataset from both studies. Diatoms, dinoflagellates, cryptomonads, and chrysophytes are grouped together as "Other eukaryotes." We calculated apparent fractionation for the cultures from Pilecky et al. (2024) from δ^2H values of C16:0 fatty acid and water in unlabeled cultures (δ^2H_{water} = -78.9 ‰), rather than using their reported $\alpha^2_{C16:0/Water}$ values, which were calculated from the slope of $\delta^2H_{C16:0}$ values plotted relative to δ^2H_{water} values. While the slope between δ^2H values of products and substrates is equivalent to α^2H when the two are separated by a single ^{2}H/^{1}H fractionating step, it differs from α^2H when the product and substrate are separated by multiple ^{2}H/^{1}H fractionating steps, as is the case for lipids relative to source water (Sessions and Hayes, 2005).

4.2 Changes in algal community composition can lead to large changes in net $^2H/^1H$ fractionation for common algal lipids

Similar to our measurements from algal batch cultures and experimental ponds, field studies of hydrogen isotope fractionation associated with common lipids in Swiss lakes have reported a wide range in $\alpha^2_{C16:0/Water}$ values, with an overall smaller range and lower values for $\alpha^2_{Phytol/Water}$ values (Ladd et al., 2017; Ladd et al., 2018). For example, in a time series of algal biomass collected from Greifensee, $\alpha^2_{C16:0/Water}$ values ranged from 0.743 to 0.891, while $\alpha^2_{Phytol/Water}$ values ranged from 0.617 to 0.668 (Ladd et al., 2017). The design of these field studies left it uncertain whether this variability in $\alpha^2_{Lipid/Water}$ values was due to variability within taxa as environmental variables such as temperature or nutrient availability changed, or if it was due to changes in community composition. Our new batch culture data demonstrates that the range in fractionation factors due to species composition alone is enough to account for natural variability in $\alpha^2_{Lipid/Water}$ values, and the taxonomic variability is an order of magnitude larger than within-species variability driven by environmental variables such as salinity, temperature, light levels, and nutrient availability (e.g., Schouten et al., 2006; Zhang and Sachs, 2007; Sachs and Kawka, 2015; van der Meer et al., 2015; Maloney et al., 2016).

The experimental pond results demonstrate how compositional variability of algal communities can lead to large shifts in $\alpha^2_{Fatty\ Acid/Water}$ values. Due to nutrient additions and interactions with keystone species, the algal community composition among the different ponds diverged, with green algae and cyanobacteria becoming much more dominant in some ponds than others (Narwani et al., 2019). Both of these taxa have higher $\alpha^2_{Fatty\ Acid/Water}$ values than other cultured algae (**Figures 1a, 5**), and it would thus be expected that $\alpha^2_{Fatty\ Acid/Water}$ values increase in ponds where they dominate, as we observed in the ponds, albeit with some scatter (**Figure 2a-c**).

592 The expected signal for changes in $\alpha^2_{Phytol/Water}$ values is more complicated, since
593 green algae had higher values than diatoms, while cyanobacteria had a non-significant
594 tendency towards lower values than diatoms (**Figure 1b**). The smaller range and minimal
595 trend in $\alpha^2_{Phytol/Water}$ values in the ponds is thus also consistent with the culturing results
596 (**Figure 2f**). In the case of stanols and sterols, $\alpha^2_{Lipid/Water}$ values for dinostanol, which is not
597 produced by green algae nor cyanobacteria, were insensitive to changing community
598 composition (**Figure 2e**), while those for stigmasterol, which is produced by cryptomonads,
599 diatoms, dinoflagellates, and green algae (Volkman, 2003; Taipale et al., 2016; Peltomaa et
600 al., 2023), decreased in the more productive ponds (**Figure 2d**), consistent with lower
601 $\alpha^2_{Sterol/Water}$ values from green algae relative to diatoms in culture (**Figure 1c**).
602 Changes in algal community composition seem more likely to explain the observed
603 changes in $\alpha^2_{Lipid/Water}$ values in the ponds than other potential explanations. Higher nutrient
604 concentrations are unlikely to explain higher $\alpha^2_{Fatty\ Acid/Water}$ values, since higher growth rates
605 and/or higher nutrient concentrations typically result in lower or constant $\alpha^2_{Lipid/Water}$ values in
606 cultured algae (Schouten et al., 2006; Z. Zhang et al., 2009; Sachs and Kawka, 2015;
607 Wolhowe et al., 2015). As such, the positive correlations between chlorophyll a
608 concentrations and $\alpha^2_{Fatty\ Acid/Water}$ values (**Figure 2)** are not indicative of a causal relationship
609 between algal growth and $\alpha^2_{Fatty\ Acid/Water}$ values, but rather an artifact of covariance with the
610 relative abundance of green algae. Second, although many common fatty acids, including
611 C16:0, are also produced by heterotrophic microbes and zooplankton, changes in relative
612 contributions from heterotrophs would be expected to produce a decrease in $\alpha^2_{Lipid/Water}$ values
613 for fatty acids in ponds with greater algal productivity. Fatty acids synthesized through
614 heterotrophic metabolisms typically have higher $\alpha^2_{Fatty\ Acid/Water}$ values than those synthesized
615 from photosynthetic products (X. Zhang et al., 2009; Osburn et al., 2011; Heinzelmann et al.,
616 2015; Cormier et al., 2018). Algal blooms are therefore expected to result in lower α^2_{Fatty}

617 $_{Acid/Water}$ values, as a higher percentage of the fatty acids will be derived from photoautotrophs
618 (Heinzelmann et al., 2016). Decreases in $\alpha^2_{Fatty\ Acid/Water}$ values during periods of increased
619 chlorophyll concentrations have in fact been observed in time series of suspended particles
620 from the water column in the North Sea (Heinzelmann et al., 2016) and in lakes from central
621 Switzerland (Ladd et al., 2017), opposite to the trend observed in the ponds with the largest
622 algal blooms.
623 Mixotrophy can also affect $\alpha^2_{Fatty\ Acid/Water}$ values (Cormier et al., 2022). Since
624 mixotrophy becomes a more dominant strategy under low nutrient conditions (Stoecker et al.,
625 2017; Wentzky et al., 2020), it should result in higher $\alpha^2_{Fatty\ acid/Water}$ values in less productive
626 ponds, the opposite of the observed trend (**Figure 2**). Additionally, the maximum effect of
627 mixotrophy within a single species across extreme conditions (green algae grown in the dark
628 on glucose compared to green algae grown in the light without glucose in the medium) is
629 only a ~ 0.040 change in $\alpha^2_{Fatty\ Acid/Water}$ values (Cormier et al. 2022), considerably smaller
630 than the ~ 0.120 variability in $\alpha^2_{Fatty\ Acid/Water}$ values among ponds (**Figure 2**). In principle,
631 mixotrophy could also affect $\alpha^2_{Dinostanol/Water}$ values, as some dinoflagellate dinostanol
632 producers are heterotrophs and/or capable of mixotrophy (Volkman, 2003); however, there
633 was much less variability in $\alpha^2_{Lipid/Water}$ values for dinostanol than for fatty acids (**Figure 2**).
634 Mixotrophy, heterotrophy, and changes in growth rate within individual taxa are therefore all
635 unlikely to explain the large variability $\alpha^2_{Fatty\ Acid/Water}$ values that occurred in our pond
636 experiment.
637
638 *4.3 Interpreting δ^2H values of multiple lipid biomarkers in sediments*
639 Lipid δ^2H values may be much more sensitive to taxonomic compositional changes in
640 the algal community than to changes in water δ^2H values, especially for compounds with a
641 diverse range of producers. As such, there is potential to develop δ^2H values of lipids as

642 paleoecological indicators, which would be particularly useful for constraining the past
643 abundance of taxonomic groups that are underrepresented in traditional microscopic
644 techniques, including most green algae, and would be complementary to pigment analyses,
645 where interpretation is challenging due to variability in the degradation rates among pigments
646 produced by different taxa. In practice, the use of lipid δ^2H values as ecological indicators
647 will be most useful when comparing changes in the relative ^2H-offsets among different
648 compounds (that is, $\delta^2H_{Lipid\ 1/Lipid\ 2}$ values), as these are insensitive to changes in water δ^2H
649 values, which will have a secondary impact on the δ^2H values of individual compounds.
650 In the pond experiment, we observed that $\delta^2H_{Lipid\ 1/Lipid\ 2}$ values for different lipid pairs
651 often changed in the way we would have predicted based on the culturing results. In
652 particular, $\delta^2H_{C16/Phytol}$ values increased in the ponds where a greater percentage of the algal
653 biovolume was from green algae and cyanobacteria (**Figure 3a**). In ponds where all or almost
654 all of the algal biovolume was from green algae and cyanobacteria, $\delta^2H_{C16/Phytol}$ values were ~
655 +300 ‰, similar to the $\delta^2H_{C16/Phytol}$ values from these two taxonomic groups in cultures
656 (**Figure 1d**). These two compounds are produced by virtually all algae, and thus may be most
657 appropriate for capturing changes in the relative contributions from different taxonomic
658 groups. Likewise, in the context of considering $\delta^2H_{Sterol/Phytol}$ and $\delta^2H_{C16/Sterol}$ values as
659 ecological indicators, it is more useful to make calculations with a sterol that is produced by
660 diverse algae, rather than a relatively source specific organism. Among the compounds we
661 were able to analyze from the ponds, stigmasterol is a relatively common sterol produced by
662 some cryptomonads, diatoms, dinoflagellates, and green algae (Volkman, 2003; Taipale et
663 al., 2016; Peltomaa et al., 2023). Based on the culturing data, $\delta^2H_{C16/Stigmasterol}$ values should
664 increase as green algal biovolume increases, exactly as observed in the ponds (**Figure 3b**). At
665 the same time, this shift should produce lower $\delta^2H_{Stigmasterol/Phytol}$ values, which we observed as
666 a non-significant trend in the ponds (**Figure 3c**).

667 Ecological effects on lipid δ^2H values have the potential to be much larger than typical
668 changes in precipitation isotopes, which at mid-latitudes vary by ~50 ‰ across large climate
669 reorganizations such as glacial-interglacial transitions (Tierney et al., 2020). Despite the
670 potential ecological complications, in many circumstances it is still possible to infer changes
671 in past water δ^2H values from sedimentary δ^2H values. In general, the more source-specific a
672 lipid biomarker is, the more likely changes in its hydrogen isotope composition are to reflect
673 changes in source water hydrogen isotopes, rather than changes in ecology. For example,
674 dinosterol δ^2H values are positively correlated with lake water and precipitation δ^2H values in
675 freshwater lakes on Pacific islands, while $C_{16:0}$ acid δ^2H values from the same sediments are
676 not (Maloney et al., 2019; Ladd et al., 2021a). The highest confidence that sedimentary δ^2H
677 signals are driven primarily by changes in precipitation δ^2H values can be achieved by
678 measuring δ^2H values of two lipids and calculating their $\delta^2H_{Lipid\ 1/Lipid\ 2}$ values (**Figure 6**). If
679 the $\delta^2H_{Lipid\ 1/Lipid\ 2}$ values are relatively stable, it is strongly suggestive that changes in the
680 individual lipid δ^2H values are primarily driven by source water δ^2H values. This is true for
681 two relatively source specific lipids, two generic lipids from different biosynthetic pathways,
682 or a combination of the two. On the other hand, fluctuating $\delta^2H_{Lipid\ 1/Lipid\ 2}$ values between
683 two lipids are indicative of change in the relative contributions from different source
684 organisms, which can either be used simply to identify non-hydrologic components of
685 sediment record, or to reconstruct algal community dynamics provided adequate background
686 on the ecological setting. Overall, measuring lipid δ^2H values from a wide range of
687 compounds within a single sediment sample, and calculating ^2H-offsets among them, offers
688 an opportunity to reconstruct changes in hydroclimate and aquatic ecology over time.

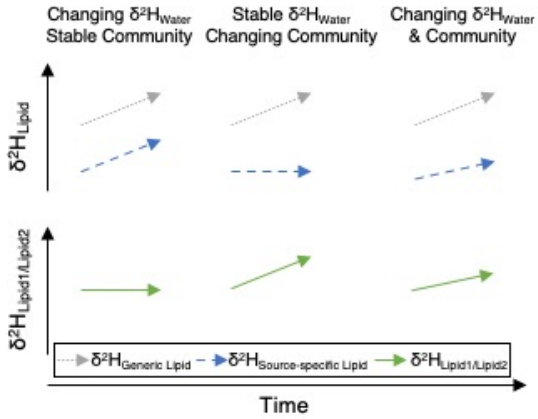

Figure 6 Schematic representation of how δ^2H_{Lipid} values and $\delta^2H_{Lipid\ 1/Lipid\ 2}$ values may change over time in response to changes in δ^2H_{Water} values and algal community composition. Positive trends in arrows are generally representative of change, and in real sediments could be negative, non-linear, or influenced by low-amplitude stochastic variability.

5. Conclusions

Hydrogen isotope fractionation during lipid synthesis varies among algal species, but these differences have not previously been systematically explored as a (paleo)ecological indicator. Here, we cultured 20 species of phytoplankton, representing cyanobacteria, diatoms, green algae, dinoflagellates, and cryptomonads, and measured the δ^2H values of their fatty acids, sterols, and phytol. We observed that δ^2H_{Lipid} values differed among taxonomic groups, and that the relative abundance of ^2H in lipids of different compound classes also displays distinct patterns among taxonomic groups. For example, diatoms produced relatively ^2H-depleted fatty acids and relatively ^2H-enriched sterols, with green algae displaying the opposite pattern. The relative ^2H-offsets between different lipids, expressed as $\delta^2H_{Lipid\ 1/Lipid\ 2}$ values, are therefore highly sensitive to taxonomic source, and can be developed as a proxy of community composition that is independent to changes in source water δ^2H values. We subsequently demonstrated how $\delta^2H_{Lipid\ 1/Lipid\ 2}$ values change with community composition through an ecosystem manipulation in 20 experimental ponds. These results can be applied to interpret sedimentary variability in δ^2H_{Lipid} values of co-occurring compounds. In sediment records, changes in δ^2H_{Lipid} values of highly source-

specific lipids, or synchronized changes in δ^2H_{Lipid} values of lipids of different compounds with diverse biological sources, can be interpreted as changes in δ^2H_{Water} values. Changes in the $\delta^2H_{Lipid\ 1/Lipid\ 2}$ values of common lipids with broad taxonomic sources, on the other hand, can be used to identify past changes in algal community composition. In this context, $\delta^2H_{C16:0/Phytol}$ values can indicate changes in the abundance of cyanobacteria and/or green algae relative to other eukaryotes, while $\delta^2H_{C16:0/Sterol}$ values can indicate changes in the abundance of green algae and dinoflagellates relative to diatoms, and $\delta^2H_{Sterol/Phytol}$ values can indicate changes in diatom abundance relative to other eukaryotic algae.

Acknowledgements

This research was funded by a US National Science Foundation postdoctoral fellowship to SNL (EAR-1452254), a Swiss National Science Foundation Eccellenza fellowship to SNL (PCEFP2_194211), and Eawag internal funds to AN, BM, and CJS. Hannele Penson assisted with sampling from experimental ponds. Serge Robert and Anton Hertler assisted with laboratory analyses of lipid samples. Daniel Montluçon measured water isotopes.

Appendix A. Supplementary Material

A list of cultured algal species and their taxonomic classification (**Table S1**) is included as a supplement to this manuscript.

Author contributions

S. Nemiah Ladd: Conceptualization, Data curation, Formal analysis, Funding acquisition, Investigation, Project coordination, Visualization, Writing – original draft, Writing – review and editing. **Daniel B. Nelson:** Conceptualization, Data curation, Formal analysis, Investigation, Writing – Review and Editing. **Blake Matthews:** Conceptualization, Funding

acquisition, Project coordination, Writing – review and editing. **Shannon Dyer:** Investigation, Writing – review and editing. **Romana Limberger:** Investigation, Writing – review and editing. **Antonia Klatt:** Data curation, Formal Analysis, Writing – review and editing. **Anita Narwani:** Data curation, Funding acquisition, Project coordination, Resources, Writing – Review and editing. **Nathalie Dubois:** Resources, Supervision, Writing – Review and Editing. **Carsten J. Schubert:** Conceptualization, Funding acquisition, Resources, Supervision, Writing – review and editing.

Data availability

All lipid and water δ^2H values generated as part of this study are available through the Dryad Digital Repository (https://doi.org/10.5061/dryad.nvx0k6f0v). Additional data from the pond experiment, including algal cell counts, biovolume, and water chemistry, is available through the Dryad Digital Repository (https://doi.org/10.5061/dryad.qv9s4mw99).

References

Archibald, J.M., 2015. Genomic perspectives on the birth and spread of plastids. Proc. Natl. Acad. Sci. U. S. A. 112, 10147-10153.

Bailleul, B., Berne, N., Murik, O., Petroutsos, D., Prihoda, J., Tanaka, A., Villanova, V., Bligny, R., Flori, S., Falconet, D., Krieger-Liszkay, A., Santabarbara, S., Rappaport, F., Joliot, P., Tirichine, L., Falkowski, P.G., Cardol, P., Bowler, C., Finazzi, G., 2015. Energetic coupling between plastids and mitochondria drives CO_2 assimilation in diatoms. Nature 524, 366–369.

Bauersachs, T., Talbot, H.M., Sidgwick, F., Sivonen, K., Schwark, L., 2017. Lipid biomarker signatures as tracers for harmful cyanobacterial blooms in the Baltic Sea. PLoS ONE 12, e0186360.

Bentlage, B., Rogers, T.S., Bachvaroff, T.R., Delwiche, C.F., 2016. Complex ancestries of isoprenoid synthesis in dinoflagellates. J. Eukaryotic Microbiol. 63, 123–137.

Bianchi, T.S., Rolff, C., Widbom, B., Elmgren, R., 2002. Phytoplankton pigments in Baltic Sea seston and sediments: seasonal variability, fluxes, and transformations. Estuarine, Coastal Shelf Sci. 55, 369–383.

Boere, A.C., Rijpstra, W.I.C., de Lange, G.J., Sinninghe Damsté, J.S., Coolen, M.J.L., 2011. Preservation potential of ancient plankton DNA in Pleistocene marine sediments. Geobiology 9, 377–393.

Casteñada, I.S., Schouten, S., 2011. A review of molecular organic proxies for examining modern and ancient lacustrine environments. Quat. Sci. Rev. 30, 2851–2891.

Chikaraishi, Y., Naraoka, H., Poulson, S.R., 2004. Hydrogen and carbon isotopic fractionations of lipid biosynthesis among terrestrial (C_3, C_4 and CAM) and aquatic plants. Phytochemistry 65, 1369–1381.

Chikaraishi, Y., Tanaka, R., Tanaka, A., Ohkouchi, N., 2009. Fractionation of hydrogen isotopes during phytol biosynthesis. Org. Geochem. 40, 569–573.

Coplen, T.B., 2011. Guidelines and recommended terms for expression of stable-isotope-ratio and gas-ratio measurement results. Rapid Commun. Mass Spectrom. 25, 2538–2560.

Cormier, M.-A., Werner, R.A., Sauer, P.E., Grocke, D.R., Leuenberger, M.C., Wieloch, T., Schleucher, J., Kahmen, A., 2018. ^{2}H-fractionations during the biosynthesis of carbohydrates and lipids imprint a metabolic signal on the δ^2H values of plant organic compounds. New Phytol. 218, 479–491.

Cormier, M.-A., Berard, J.-B., Bougaran, G., Tureman, C.N., Mayer, D.J., Lampitt, R.S., Kruger, N.J., Flynn, K.J., Rickaby, R.E.M., 2022. Deuterium in marine organic biomarkers: toward a new tool for quantifying aquatic mixotrophy. New Phytol. 234, 776–782.

Diaz, R.J., Rosenberg, R., 2008. Spreading dead zones and consequences for marine ecosystems. Science 321, 926–929.

Disch, A., Schwender, J., Müller, C., Lichtenthaler, H.K., Rohmer, M., 1998. Distribution of the mevalonate and glyceraldehyde phosphate/pyruvate pathways for isoprenoid biosynthesis in unicellular algae and the cyanobacterium *Synechocystis* PCC 6714. Biochem. J. 333, 381–388.

Dixit, A.S., Dixit, S.S., Smol, J.P., 1992. Algal microfossils provide high temporal resolution of environmental trends. Water, Air, Soil Pollut. 62, 75–87.

Gosling, W.D., Sear, D.A., Hassall, J.D., Langdon, P.G., Bönnen, M.N.T., Driessen, T.D., van Kemenade, Z.R., Noort, K., Leng, M.J., Croudace, I.W., Bourne, A.J., McMichael, C.N.H., 2020. Human occupation and ecosystem change on Upolu (Samoa) during the Holocene. J. Biogeogr. 47, 600–614.

Guillard, R.R.L., Lorenzen, C.J., 1972. Yellow-green algae with chlorophyllide c. J. Phycol. 8, 10–14.

Haas, M., Baumann, F., Castella, D., Haghipour, N., Reusch, A., Strasser, M., Eglington, T.I., Dubois, N., 2019. Roman-driven cultural eutrophication of Lake Murten, Switzerland. Earth Planet. Sci. Lett. 505, 110–117.

Heinzelmann S.M., Villanueva L., Sinke-Schoen D., Sinninghe Damsté J.S., Schouten S., van der Meer M.T.J., 2015. Impact of metabolism and growth phase on the hydrogen isotopic composition of microbial fatty acids. Front. Microbiol. 6, 408.

Heinzelmann S.M., Bale N.J., Villanueva L., Sinke-Schoen D., Philippart C.J.M., Sinninghe Damsté J.S., Smede J., Schouten S. van der Meer M.T.J., 2016. Seasonal changes in the D/H ratio of fatty acids of pelagic microorganisms in the coastal North Sea. Biogeosciences 13, 5527–5539.

Hemmerlin A., Harwood J.L., Bach, T.J., 2012. A raison d'être for two distinct pathways in the early steps of plant isoprenoid biosynthesis? Prog. Lipid Res. 51, 95–148.

Hixon, S.M., Arts, M.T., 2016. Climate warming is predicted to reduce omega-3, long-chain, polyunsaturated fatty acid production in phytoplankton. Global Change Biol. 22, 2744–2755.

Huang Y., Shuman B., Wang Y., Webb III T., 2004. Hydrogen isotope ratios of individual lipids in lake sediments as novel tracers of climatic and environmental change: a surface sediment test. J. Paleolimnol. 31, 363–375.

819 Huisman, J., Codd, G.A., Paerl, H.W., Ibelings, B.W., Verspagen, J.M.H., Visser, P.M.,
820 2018. Cyanobacterial blooms. Nat. Rev. Microbiol. 16, 471–483.
821 Kirkpatrick, J.B., Walsh, E.A., D'Hondt, S., 2016. Fossil DNA persistence and decay in
822 marine sediment over hundred-thousand-year to million-year time scales. Geology 44,
823 615–618.
824 Krentscher, C., Dubois, N., Camperio, G., Prebble, M., Ladd S.N., 2019. Palmitone as a
825 potential species-specific biomarker for the crop plant taro (*Colocasia esculenta* Schott)
826 on remote Pacific islands. Org. Geochem. 132, 1–10.
827 Kreuzwieser, J., Meischner, M., Grün, M., Yáñez-Serrano, A.M., Fasbender, L., Werner, C.,
828 2021. Drought affects carbon partitioning into volatile organic compound
829 biosynthesis in Scots pine needles. New Phytol. 232, 1930–1943.
830 Ladd, S.N., Dubois, N., and Schubert, C.J., 2017. Interplay of community dynamics,
831 temperature, and productivity on the hydrogen isotope signatures of lipid biomarkers.
832 Biogeosciences 14, 3979–3994.
833 Ladd, S.N., Nelson, D.B., Schubert, C.J., Dubois, N., 2018. Lipid compound classes display
834 diverging hydrogen isotope responses in lakes along a nutrient gradient. Geochim.
835 Cosmochim. Acta 237, 103–119.
836 Ladd, S.N., Maloney, A.E., Nelson, D.B., Prebble, M., Camperio, G., Sear, D.A., Hassall, J.,
837 Langdon, P.G., Sachs, J.P., Dubois, N., 2021. Leaf wax hydrogen isotopes as a
838 hydroclimate proxy in the tropical Pacific. J. Geophys. Res.: Biogeosci. 126,
839 e2020JG005891.
840 Ladd, S.N., Nelson, D.B., Bamberger, I., Daber, L.E., Kreuzwieser, J., Kahmen, A., Werner,
841 C., 2021b. Metabolic exchange between pathways for isoprenoid synthesis and
842 implications for biosynthetic hydrogen isotope fractionation. New Phytol. 231, 1708–
843 1719
844 Ladd, S.N., Daber, L.E., Bamberger, I., Kübert, A., Kreuzwieser, J., Purser, G., Ingrisch, J.,
845 Deleeuw, J., van Haren, J., Meredith, L.K., Werner, C., 2023. Leaf-level metabolic
846 changes in response to drought affect daytime CO_2 emission and isoprenoid synthesis
847 pathways. Tree Physiol. 43, 1917–1932.
848 Leavitt, P.R., Findlay, D.L., 1994. Comparison of fossil pigments with 20 years of
849 phytoplankton data from eutrophic Lake 227, Experimental Lakes Area, Ontario. Can.
850 J. Fish. Aquat. Sci. 51, 2286–2299.
851 Leavitt P.R., Hodgson D.A., 2002. Sedimentary pigments, in: Smol J.P., Birks H.J.B., Last
852 W.M., Bradley R.S., Alverson K. (Eds.) Tracking Environmental Change Using Lake
853 Sediments. Developments in Paleoenvironmental Research, vol 3. Springer,
854 Dordrecht, Netherlands, pp. 295–325.
855 Lichtenthaler, H.K., 1999. The 1-Deoxy-D-Xylulose-5-Phosphate pathway of isoprenoid
856 biosynthesis in plants. Ann. Rev. Plant Phys. 50, 47–65.
857 Livingstone, D., Jaworski, G.H.M., 1980. The viability of akinetes of blue-green algae
858 recovered from the sediments of R ostherne M ere. Br. Phycol. J. 15, 357–364.
859 Lotter, A.F., 1998. The recent eutrophication of Baldeggersee (Switzerland) as assessed by
860 fossil diatom assemblages. The Holocene 8, 395–405.
861 Lürig, M.D., Narwani, A., Penson, H., Wehrli, B., Spaak, P., Matthews, B., 2021. Non-
862 additive effects of foundation species determine the response of aquatic ecosystems to
863 nutrient perturbation. Ecology 102, e03371.
864 Maloney, A.E., Shinneman, A.L., Hemeon, K., Sachs, J.P., 2016. Exploring lipid ^{2}H/^{1}
865 H fractionation mechanisms in response to salinity with continuous cultures of the
866 diatom *Thalassiosira pseudonana*. Org. Geochem. 101, 154–165.
867 Maloney, A.E., Nelson, D.B., Richey, J.N., Prebble, M., Sear, D.A., Hassell, J.D., Langdon,
868 P.G., Croudace, I.W., Zawadzki, A., Sachs, J.P., 2019. Reconstructing precipitation in

the tropical South Pacific from dinosterol $^{2}H/^{1}H$ ratios in lake sediment. Geochim. Cosmochim. Acta 245, 190–206.
Markelov I., Couture, R.-M., Fischer, R., Haande, S., Van Cappellen, P., 2019. Coupling water column and sediment biogeochemical dynamics: modeling internal Phosphorus lading, climate change responses, and mitigation measures in Lake Vansjo, Norway. J. Geophys. Res.: Biogeosci. 124, 3847–3866.
McGowan, S., Barker, P., Haworth, E.Y., Leavitt, P.R., Maberly, S.C., Pates, J., 2012. Humans and climate as drivers of algal community change in Windermere since 1850. Freshwater Biol. 57, 260–277.
Meyers, P.A., 1997. Organic geochemical proxies of paleoceanographic, paleolimnologic, and paleoclimatic processes. Org. Geochem. 27, 213–250.
Monchamp, M., Spaak, P., Domaizon, I., Dubois, N., Bouffard, D., Pomati, F., 2018. Homogenization of lake cyanobacterial communities over a century of climate change and eutrophication. Nat. Ecol. Evol. 2, 317–324.
Naeher, S., Smittenberg, R.H., Gilli, A., Kirilova, E.P., Lotter, A., Schubert, C.J., 2012. Impact of recent lake eutrophication on microbial community change as revealed by high resolution lipid biomarkers in Rotsee (Switzerland). Org. Geochem. 49, 86–95.
Narwani, A., Reyes, M., Pereira, A.L., Penson, H., Dennis, S.R., Derrer, S., Spaak, P., Matthews, B., 2019. Interactive effects of foundation species on ecosystem functioning and stability in response to disturbance. Proc. R. Soc. B 286, 20191857.
Nelson D.B., Sachs J.P., 2014. The influence of salinity on D/H fractionation in dinosterol and brassicasterol from globally distributed saline and hypersaline lakes. Geochim. Cosmochim. Acta 133, 325–339.
Nwosi, E.C., Brauer, A., Monchamp, M.-E., Pinkerneil, S., Bartholomäus, A., Theuerkauf, M., Schmidt, J.-P., Stoof-Leichsenring, K.R., Wietelmann, T., Kaiser, J., Wagner, D., Liebner, S., 2023. Early human impact on lake cyanobacteria revealed by a Holocene record of sedimentary ancient DNA. Commun. Biol. 6, 72.
Opitz, S., Nes, W.D., Gershenzon, J., 2014. Both methylerythritol phosphate and mevalonate pathways contribute to biosynthesis of each of the major isoprenoid classes in young cotton seedlings. Phytochemistry 98, 110–119.
Osburn M.R., Sessions A.L., Pepe-Ranney C., Spear J.R., 2011. Hydrogen-isotopic variability in fatty acids from Yellowstone National Park hot spring microbial communities. Geochim. Cosmochim. Acta 75, 4830–4845.
Pawlowski, J., Kelly-Quinn, M., Altermatt, F., Apothéloz-Perret-Gentil, L., Beja, P., Boggero, A., Borja, A., Bouchez, A., Cordier, T., Domaizon, I., Feio, M.J., Filipe, A.F., Fornaroli, R., Graf, W., Herder, J., van der Hoorn, B., Jones, J.I., Sagova-Mareckova, M., Moritz, C., Barquín, J., Piggott, J.J., Pinna, M., Rimet, F., Rinkevich, B., Sousa-Santos, C., Specchia, V., Trobajo, R., Vasselon, V., Vitecek, S., Zimmermann, J. Weigand, A., Leese, F., Kahlert, M.. 2018. The future of biotic indices in the ecogenomic era: Integrating (e)DNA metabarcoding in biological assessment of aquatic ecosystems. Sci. Total Environ. 637-638, 1295–1310.
Peltomaa, E., Asikainen, H., Blomster, J., Pakkanen, H., Rigaud, C., Salmi, P., Taipale, S., 2023. Phytoplankton group identification with chemotaxonomic biomarkers: In combination they do better. Phytochemistry 209, 113624.
Pilecky, M., Kainz, M.J., Wassenaar, L.I., 2024. Exploring hydrogen isotope fractionation in lipid biomolecules of freshwater algae: implications for ecological and

paleoenvironmental studies. Isotopes Environ. Health Stud. DOI: 10.1080/10256016.2024.2419880

Rabalais, N.N., Diaz, R.J., Levin, L.A., Turner, R.E., Gilbert, D., Zhang, J., 2010. Dynamics and distribution of natural and human-caused hypoxia. Biogeosciences 7, 585–619.

Reuss, N., Conley, D.J., Bianchi, T.S., 2005. Preservation conditions and the use of sedimentary pigments as a tool for recent ecological reconstruction in four Northern European estuaries. Mar. Chem. 95, 283–302.

Rhim, J.H., Kopf, S., McFarlin, J., Maloney, A.E., Batther, H., Harris, C.M., Zhou, A., Feng, X., Weber, Y., Hoeft-McCann, S., Pearson, A., Leavitt, W.D., in press . Metabolic imprints in the hydrogen isotopes of *Archaeoglobus fulgidus* tetraether lipids. Geochim. Cosmochim. Acta, doi: 10.1016/j.gca.2024.09.032

Sachs, J.P., Kawka, O.E., 2015. The influence of growth rate on ^{2}H/^{1}H fractionation in continuous cultures of the coccolithophorid *Emiliania huxleyi* and the diatom *Thalassiosira pseudonana*. PloS ONE 10, e0141643.

Sachs, J.P., Maloney, A.E., Gregersen, J., Paschall, C., 2016. Effect of salinity on ^{2}H/^{1}H fractionation in lipids from continuous cultures of the coccolithophorid *Emiliania huxleyi*. Geochim. Cosmochim. Acta 189, 96–109.

Sachs, J.P., Maloney, A.E., Gregersen, J., 2017. Effect of light on ^{2}H/^{1}H fractionation in lipids from continuous cultures of the diatom *Thalassiosira pseudonana*. Geochim. Cosmochim. Acta 209, 204–215.

Sachse, D., Radke, J., Gleixner, G., 2004. Hydrogen isotope ratios of recent lacustrine sedimentary *n*-alkanes record modern climate variability. Geochim. Cosmochim. Acta 68, 4877–4889.

Sachse, D., Sachs, J., 2008. Inverse relationship between D/H fractionation in cyanobacterial lipids and salinity in Christmas Island saline ponds. Geochim. Cosmochim. Acta 72, 793–806.

Sachse, D., Billault, I., Bowen, G.J., Chikaraishi, Y., Dawson, T.E., Feakins, S.J., Freeman, K.H., Magill, C.R., McInerney, F.A., Van der Meer, M.T.J., Polissar, P., Robins, R.J., Sachs, J.P., Schmidt, H., Sessions, A.L., White, J.W.C., West, J.B., Kahmen, A., 2012. Molecular paleohydrology: interpreting the hydrogen-isotope composition of lipid biomarkers from photosynthesizing organisms. Annu. Rev. Earth Planet. Sci. 40, 221–249.

Schimmelmann, A., Sessions, A.L., Mastalerz, M., 2006. Hydrogen isotopic (D/H) composition of organic matter during diagenesis and thermal maturation. Annu. Rev. Earth Planet. Sci. 34, 501–533.

Schmidt, H.L., Werner, R., Eisenreich, W., 2003. Systematics of ^{2}H patterns in natural compounds and its importance for the elucidation on biosynthetic pathways. Phytochem. Rev. 2, 61–85.

Schouten, S., Ossebaar, J., Schreiber, K., Kienhuis, M.V.M., Langer, G., Benthien, A., Bijma, J., 2006. The effect of temperature, salinity and growth rate on the stable hydrogen isotopic composition of long chain alkenones produced by *Emiliania huxleyi* and *Gephyrocapsa oceanica*. Biogeosciences 3, 113–119.

Schubert, C.J., Villanueva, J., Calvert, S.E., Cowie, G.L., von Rad, U., Schulz, H., Berner, U., Erlenkeuser, H., 1998. Stable phytoplankton community structure in the Arabian Sea over the past 200,000 years. Nature 394, 563-566.

Schwab, V.F., Garcin, Y., Sachse, D., Todou, G., Séné, O., Onana, J., Achoundong, G., Gleixner, G., 2015. Dinosterol δD values in stratified tropical lakes (Cameroon) are affected by eutrophication. Org. Geochem. 88, 35–49.

963 Schwender, J., Seemann, M., Lichtenthaler, H.K., Rohmer, M., 1996. Biosynthesis of
964 isoprenoids (carotenoids, sterols, prenyl side–chains of chlorophylls and
965 plastoquinone) via a novel pyruvate/glyceraldehyde 3–phosphate non–mevalonate
966 pathway in the green alga *Scenedesmus obliquus*. Biochem. J. 316, 73–80.
967 Sessions, A.L., Burgoyne, T.W., Schimmelmann, A., Hayes, J.M., 1999. Fractionation of
968 hydrogen isotopes in lipid biosynthesis. Org. Geochem. 30, 1193–1200.
969 Sessions, A.L., Hayes, J.M., 2005. Calculation of hydrogen isotopic fractionations in
970 biogeochemical systems. Geochim. Cosmochim. Acta 69, 593–597.
971 Sessions, A.L., 2006. Seasonal changes in D/H fractionation accompanying lipid biosynthesis
972 in *Spartina alterniflora*. Geochim. Cosmochim. Acta 70, 2153–2162.
973 Stoecker, D.K., Hansen, P.J., Caron, D.A., Mitra, A., 2017. Mixotrophy in the marine plankton.
974 Annu. Rev. Mar. Sci. 9, 311–335.
975 Stoermer, E.F., Wolin, J.A., Schelske, C.L., Conley, D.J., 1985. An assessment of ecological
976 changes during the recent history of Lake Ontario based on siliceous algal microfossils
977 preserved in sediments. J. Phycol. 21, 257–276.
978 Stoof-Leichsenring, K.R., Herzschuh, U., Pestryakova, L.A., Klemm, J., Epp, L.S.,
979 Tiedemann, R., 2015. Genetic data from algae sedimentary DNA reflect the influence
980 of environment over geography. Sci. Rep. 5, 12924.
981 Strivins, N., Soininen, J., Tonno, I., Freiberg, R., Veski, S., Kisand, V., 2018. Towards
982 understanding the abundance of non-pollen palynomorphs: a comparison of fossil
983 algae, algal pigments and sedaDNA from temperate northern lake sediments. Rev.
984 Palaeobot. Palynol. 249, 9–15.
985 Taipale, S.J., Hiltunen, M., Vuorio, K., Peltomaa, E., 2016. Suitability of phytosterols
986 alongside fatty acids as chemotaxonomic biomarkers for phytoplankton. Front. Plant
987 Sci. 7, 212.
988 Thorpe, A.C., Mackay, E.B., Goodall, T., Bendle, J.A., Thackeray, S.J., Maberly, S.C., Read,
989 D.S., 2024. Evaluating the use of lake sedimentary DNA in palaeolimnology: A
990 comparison with long-term microscopy-based monitoring of the phytoplankton
991 community. Mol. Ecol. Resour. 24, e13903.
992 Tierney, J.E., Zhu, J., King, J., Malevich, S.B., Hakim, G.J., Poulsen, C.J., 2020. Glacial
993 cooling and climate sensitivity revisited. Nature 584, 569–573.
994 van der Meer M.T.J., Benthien A., French K.L., Epping E., Zondervan I., Reichart G.J.,
995 Bijma J., Sinninghe Damsté J.S., Schouten,S. 2015. Large effect of irradiance on
996 hydrogen isotope fractionation of alkenones in *Emiliania huxleyi*. Geochim.
997 Cosmochim. Acta 160, 16–24.
998 Vasselon, V., Bouchez, A., Rimet, F., Jacquet, S., Trobajo, R., Corniquel, K., Domaizon, I.,
999 2018. Avoiding quantification bias in metabarcoding: Application of a cell biovolume
1000 correction factor in diatom molecular biomonitoring. Methods Ecol. Evol. 9, 1060–
1001 1069.
1002 Volkman J.K., 2003. Sterols in microorganisms. Appl. Microbiol. Biotechnol. 60, 495–506.
1003 Weiss, G.M., Schouten, S., Sinninghe Damsté, J.S., van der Meer, M.T.J., 2019. Constraining
1004 the application of hydrogen isotopic composition of alkenones as a salinity proxy
1005 using marine surface sediments. Geochim. Cosmochim. Acta 250, 34–48.
1006 Wentzky, V.C., Tittel, J., Jäger, C.G., Bruggeman, J., Rinke, K., 2020. Seasonal succession
1007 of functional traits in phytoplankton communities and their interaction with trophic
1008 state. J. Ecol. 108, 1649–1663.

Wijker, R.S., Sessions, A.L., Fuhrer, T., Phan, M., 2019. $^{2}H/^{1}H$ variation in microbial lipids is controlled by NADPH metabolism. Proc. Natl. Acad. Sci. U. S. A. 116, 12173–12182.

Witkowski, C.R., Weijers, J.W.H., Blais, B., Schouten, S., Sinninghe Damsté, J.S., 2018. Molecular fossils from phytoplankton reveal secular P_{CO2} trend over the Phanerozoic. Sci. Adv. 4, eaat4556.

Wolhowe, M.D., Prahl, F.G., Langer, G., Oviedo, A.M., Ziveri, P., 2015. Alkenone δD as an ecological indicator: A culture and field study of physiologically-controlled chemical and hydrogen-isotopic variation in C_{37} alkenones. Geochim. Cosmochim. Acta 162, 166–182.

Yáñez–Serrano, A.M., Mahlau, L., Fasbender, L., Byron, J., Williams, J., Kreuzwieser, J., Werner, C., 2019. Heat stress increases the use of cytosolic pyruvate for isoprene biosynthesis. J. Exp. Bot. 70, 5827–5838.

Zhang, Z., Sachs, J.P., 2007. Hydrogen isotope fractionation in freshwater algae: 1. Variations among lipids and species. Org. Geochem. 38, 582–608.

Zhang, X., Gillespie, A., Sessions, A.L., 2009. Large D/H variations in bacterial lipids reflect central metabolic pathways. Proc. Natl. Acad. Sci. U. S. A. 106, 12580–12586.

Zhang, Z., Sachs, J.P., Marchetti, A., 2009. Hydrogen isotope fractionation in freshwater and marine algae: II. Temperature and nitrogen limited growth rate effects. Org. Geochem. 40, 428–439.

Zhang, Z., Nelson, D.B., Sachs, J.P., 2014. Hydrogen isotope fractionation in algae: III. Theoretical interpretations. Org. Geochem. 75, 1–7.

Zhou, Y., Grice, K., Chikaraishi, Y., Stuart-Williams, H., Farquhar, G.D., Ohkouchi, N., 2011. Temperature effect on leaf water deuterium enrichment and isotopic fractionation during leaf lipid biosynthesis: Results from controlled growth of C_3 and C_4 land plants. Phytochemistry 72, 207–213.

Zulu, N.N., Zienkiewicz, K., Vollheyde, K., Feussner, I., 2018. Current trends to comprehend lipid metabolism in diatoms. Prog. Lipid Res. 70, 1–16.

Supplementary Material for: Taxon-specific hydrogen isotope signals in cultures and mesocosms facilitate ecosystem and hydroclimate reconstruction

S. Nemiah Ladd[a, b]*, Daniel B. Nelson[b, c], Blake Matthews[d], Shannon Dyer[b], Romana Limberger[e,f], Antonia Klatt[a], Anita Narwani[g], Nathalie Dubois[h, i], Carsten J. Schubert[b, j]

[a] University of Basel, Department of Environmental Sciences, Basel, Switzerland

[b] Swiss Federal Institute of Aquatic Science and Technology (EAWAG), Department of Surface Waters – Research and Management, Kastanienbaum, Switzerland

[c] University of Basel, Department of Environmental Sciences – Botany, Basel, Switzerland

[d] Swiss Federal Institute of Aquatic Science and Technology (EAWAG), Department of Fish Ecology and Evolution, Kastanienbaum, Switzerland

[e] Swiss Federal Institute of Aquatic Science and Technology (EAWAG), Department of Aquatic Ecology, Kastanienbaum, Switzerland

[f] University of Zurich, Department of Evolutionary Biology and Environmental Studies, Zurich, Switzerland

[g] Swiss Federal Institute of Aquatic Science and Technology (EAWAG), Department of Aquatic Ecology, Dübendorf, Switzerland

[h] Swiss Federal Institute of Aquatic Science and Technology (EAWAG), Department of Surface Waters – Research and Management, Dübendorf, Switzerland

[i] Swiss Federal Institute of Technology (ETH-Zürich), Department of Earth Sciences, Zürich, Switzerland

[j] Swiss Federal Institute of Technology (ETH-Zürich), Department of Environmental Systems Science, Zürich, Switzerland

Contents:

Table S1: Cultured algal species and taxonomic classifications

Species	Group	Class	Source and Strain	Number of replicate cultures
Achnanthes sp.	diatoms	Bacillariophyceae	CCAC 2681 B	3
Aphanizomenon flos-aquae	cyanobacteria	Cyanophyceae	NIVA 693	3
Aphanothece clathrata	cyanobacteria	Cyanophyceae	SAG 23.99	3
Asterionella formosa	diatoms	Bacillariophyceae	NIVA BAC-3	2
Botryococcus braunii-1	green algae	Trebouxiophyceae	SAG 2532	3
Botryococcus braunii-2	green algae	Trebouxiophyceae	SAG 30.81	3
Chlamydomonas reinhardtii	green algae	Chlorophyceae	CC 1690	3
Cosmarium botrytis	green algae	Conjugatophyceae	SAG 136.80	3
Cryptomonas ovata	Cryptomonads	Cryptophyceae	SAG 980-1	2
Cyclotella meneghiniana	diatoms	Mediophyceae	Leah Lewington-Pearce	2
Cystodinium spec.	dinoflagellates	Dinophyta	SAG 59.87	2
Eudorina unicocca	green algae	Chlorophyceae	SAG 49.91	3
Microcystis aeruginosa	cyanobacteria	Cyanophyceae	PCC 7806	2
Peridinium spec.	dinoflagellates	Dinophyta	SAG 2017	2
Scenedesmus acuminatus	green algae	Chlorophyceae	SAG 38.81	3
Stephanodiscus minutulus	diatoms	Bacillariophyceae	SAG 49.91	3
Synechococcus	cyanobacteria	Cyanophyceae	CCAP 1479110	5
Synedra rumpens var. familiaris	diatoms	Bacillariophyceae	NIVA BAC-18	2
Tabellaria sp.	diatoms	Bacillariophyceae	CCAC 3717 B	3
Volvox aureus	green algae	Chlorophyceae	SAG 88-1	3

Table S2: Relative retention times and prominent ions from acetylated sterols identified in experimental ponds and batch cultures

Relative Retention Time[1]	Systematic name	Trivial name	Base Peak	Other prominent M+ ions
0.0	Cholest-5-en-3β-ol	Cholesterol	368	55, 105, 146, 247
0.2	Cholestan-3β-ol	Cholestanol	215	81, 147, 253, 355, 429
0.8	(22E)-ergosta-5,22-dien-3β-ol	Brassicasterol	380	69, 105, 145, 255
1.1	Campest-5-en-3β-ol	Campesterol	384	215, 276, 369
1.6	(22E)-ergosta-5,7,22-trien-β-ol	Ergosterol	382	105, 147, 255
1.8	(22E)-5α-poriferasta-7,22-dien-3β-ol	Chondrillasterol	95	55, 135, 271, 394, 456
2.1	(24E)-stigmasta-5,22-dien-3β-ol	Stigmasterol	394	81, 145, 255
2.5	5α-ergost-7-en-3β-ol	Fungisterol	255	57, 105, 213, 382, 442
3.0	5α-poriferast-7-en-3β-ol	22-dehydrochondrillasterol	313	81, 147, 255, 396, 454
3.2	4α-23,24-trimethyl-5α-cholest-22E-en-3β-ol	Dinosterol	69	271, 329, 358, 408
3.9	Stigmasta-5-en-3β-ol	Sitosterol	396	81, 105, 145k
4.2	4α-23,24-trimethyl-5α-cholestan-3β-ol	Dinostanol	229	95, 290, 412, 472

[1]Minutes after cholesterol with GC column and method described in section 2.3